


Naphthoquinoxaline metabolite of mitoxantrone is less cardiotoxic than the parent compound and it can be a more cardiosafe drug in anticancer therapy

A. Reis-Mendes¹ · A. S. Gomes^{2,4} · R. A. Carvalho³ · F. Carvalho¹ · F. Remião¹ · M. Pinto^{4,5} · M. L. Bastos¹ · E. Sousa^{4,5} · V. M. Costa¹ 

Received: 13 May 2016 / Accepted: 24 August 2016 / Published online: 14 September 2016
© Springer-Verlag Berlin Heidelberg 2016

Abstract Mitoxantrone (MTX) is an antineoplastic agent used to treat several types of cancers and on multiple sclerosis, which shows a high incidence of cardiotoxicity. Still, the underlying mechanisms of MTX cardiotoxicity are poorly understood and the potential toxicity of its metabolites scarcely investigated. Therefore, this work aimed to synthesize the MTX-naphthoquinoxaline metabolite (NAPHT) and to compare its cytotoxicity to the parent compound in 7-day differentiated H9c2 cells using pharmacological relevant concentrations (0.01–5 μ M). MTX was more toxic in equivalent concentrations in all cytotoxicity tests performed [3-(4,5-dimethylthiazol-2-yl)-2,5-diphenyl tetrazolium bromide reduction, neutral red uptake, and lactate dehydrogenase release assays] and times tested (24 and 48 h). Both MTX and NAPHT significantly decreased

mitochondrial membrane potential in 7-day differentiated H9c2 cells after a 12-h incubation. However, energetic pathways were affected in a different manner after MTX or NAPHT incubation. ATP increased and lactate levels decreased after a 24-h incubation with MTX, whereas for the same incubation time and concentrations, NAPHT did not cause any significant effect. The increased activity of ATP synthase seems responsible for MTX-induced increases in ATP levels, as oligomycin (an inhibitor of ATP synthase) abrogated this effect on 5 μ M MTX-incubated cells. 3-Methyladenine (an autophagy inhibitor) was the only molecule to give a partial protection against the cytotoxicity produced by MTX or NAPHT. To the best of our knowledge, this was the first broad study on NAPHT cardiotoxicity, and it revealed that the parent drug, MTX, caused a higher disruption in the energetic pathways in a cardiac model *in vitro*, whereas autophagy is involved in the toxicity of both compounds. In conclusion, NAPHT is claimed to largely contribute to MTX-anticancer properties; therefore, this metabolite should be regarded as a good option for a safer anticancer therapy since it is less cardiotoxic than MTX.

Part of this article has been taken from the first author's thesis entitled "The synthesis and *in vitro* toxicological evaluation of the mitoxantrone naphthoquinoxaline metabolite: a comparative study with the parent drug" printed last September 2014. The thesis document is available online at the university repository (available at <http://repositorio-aberto.up.pt/bitstream/10216/77095/2/103849.pdf>).

✉ A. Reis-Mendes
afreis.mendes@gmail.com

✉ V. M. Costa
veramcosta@ff.up.pt

¹ UCIBIO-REQUIMTE (Rede de Química e Tecnologia), Laboratório de Toxicologia, Departamento de Ciências Biológicas, Faculdade de Farmácia, Universidade do Porto, Rua de Jorge Viterbo Ferreira, 228, 4050-313 Porto, Portugal

² UCIBIO-REQUIMTE, Laboratory of Microbiology, Department of Biological Sciences, Faculty of Pharmacy, University of Porto, Rua de Jorge Viterbo Ferreira 228, 4050-313 Porto, Portugal

³ Centre for Functional Ecology, Department of Life Sciences, Faculty of Sciences and Technology, University of Coimbra, Coimbra, Portugal

⁴ Lab. Química Orgânica e Farmacêutica, Dep. Química, Faculdade de Farmácia, U. Porto, Porto, Portugal

⁵ CIIMAR – Interdisciplinary Centre of Marine and Environmental Research, Porto, Portugal

Keywords Mitoxantrone · Autophagy · Naphthoquinoxaline · Differentiated H9c2 cells · Cardiotoxicity

Abbreviations

ATP	Adenosine triphosphate
DiO ₆	3,3'-Dihexyloxacarboyanine iodide
DMEM	Dulbecco's modified eagle medium
DMSO	Dimethyl sulphoxide
FBS	Foetal bovine serum
FU	Fluorescence units
h	Hours
HPLC	High-performance liquid chromatography
HRP	Horse radish peroxidase
<i>k</i>	Retention factor
LDH	Lactate dehydrogenase
min	Minutes
MTT	3-(4,5-Dimethylthiazol-2-yl)-2,5-diphenyl tetrazolium bromide
MTX	Mitoxantrone
<i>m</i>	Multiplet
NADH	Nicotinamide adenine dinucleotide reduced form
NAPHT	Naphthoquinoxaline
NR	Neutral red
NMR	Nuclear magnetic resonance
PBS	Phosphate-buffered saline
RA	Retinoic acid
<i>s</i>	Singlet
SD	Standard deviation
SDS	Sodium dodecyl sulphate
<i>t</i>	Triplet
TLC	Thin-layer chromatography
UV	Ultraviolet

Introduction

Cancer is one of the most concerning health issues worldwide. Still, it is no longer considered a death sentence, as the 5-year survival has been largely increasing in the last few years (Allemani et al. 2015). Over 3.45 million new cases of cancer (excluding non-melanoma skin cancers) and 1.75 million deaths were registered in Europe in 2012, with breast and prostate cancers counting for more than 800,000 new cases (Ferlay et al. 2013). Mitoxantrone (MTX) is an antineoplastic agent belonging to the family of the synthetic anthracenediones (Ehninger et al. 1990), and it was originally synthesized in 1979. The main difference in the chemical structure of MTX compared with anthracyclines is the replacement of the amino sugar on the anthracyclines with aminoalkylalcohol chains (Pratt et al. 1986). The synthesis of MTX aimed to create a molecule with the same

anticancer efficacy of doxorubicin, but without its cardiotoxic effects. Even so, clinical data have demonstrated that the cardiotoxicity of MTX is still a major concern for patients receiving intensive and/or prolonged therapy with this anticancer agent (Avasarala et al. 2003; Coleman et al. 1984; Ehninger et al. 1990; Seiter 2005). Currently, the recommended maximum lifetime cumulative dose of MTX is 140 mg/m², with 2.6–13 % of patients developing cardiac toxicity at this or higher cumulative doses (Seiter 2005). The clinical cardiotoxicity of MTX includes decreased left ventricular ejection fraction, congestive heart failure, ischaemic chest pain, arrhythmias, and conduction abnormalities on the electrocardiogram (Albini et al. 2010; Carver and Desai 2010; Menna et al. 2008). So far, the exact mechanisms of cardiotoxicity have been unknown and pharmacological preventive therapy does not exist.

The metabolism of several anticancer drugs seems to have an important role in their cardiotoxicity. Metabolites of doxorubicin, cyclophosphamide, and 5-fluorouracil have known cardiotoxic properties, as demonstrated both in *in vivo* and in *in vitro* models (Reis-Mendes et al. 2015). Although the role of metabolism on MTX cardiotoxicity is still poorly understood, we have previously demonstrated that MTX metabolism is partially responsible for its cardiotoxicity in non-differentiated H9c2 cells (Rossato et al. 2013a). The structure of the toxic metabolite (or metabolites) was not identified in that work. Only 20–32 % of the administered dose of MTX is excreted within the first 5 days (urine 6–11 %, faeces 13–25 %). From the material recovered in the urine, 65 % is unchanged MTX and the remaining 35 % are MTX metabolites. The major MTX metabolites isolated from the urine of MTX-treated patients are mono- and dicarboxylic acids, resulting from oxidation of the terminal hydroxyl groups on the side chains (Blanz et al. 1991; Chiccarelli et al. 1986). These metabolites were tested for their anticancer properties, and they were ineffective against P388 leukaemia in mice (Chiccarelli et al. 1986). Another important MTX metabolite is its cyclic metabolite, a naphthoquinoxaline (NAPHT) that is a product of the biotransformation of MTX *in vivo* in humans, pigs, and rats (Blanz et al. 1991). Studies suggest that this metabolite has a significant role in the pharmacological anticancer activity of MTX (Feofanov et al. 1997b; Mewes et al. 1993; Panousis et al. 1994, 1997). Moreover, NAPHT was found in the heart of male Wistar rats 24 h after a single 7.5 mg/kg MTX administration (Rossato et al. 2013a), thus demonstrating that this metabolite can be retained in the heart, as it happens with MTX (Ehninger et al. 1990). So far, its cardiotoxic potential has not been thoroughly evaluated. To the best of our knowledge, only one study was performed with this metabolite in neonatal cardiomyocytes and limited data were obtained (Shipp et al. 1993), not allowing strong and translational conclusions regarding its role on MTX-induced cardiotoxicity.

As the data concerning MTX and its metabolites are scarce, this work aimed to compare the cytotoxicity of MTX and its metabolite NAPHT, obtained by chemical synthesis, in an *in vitro* cardiac model, differentiated H9c2 cells and to determine whether that metabolite is or not a major contributor for MTX's cardiotoxicity.

Materials and methods

Materials

The rat cardiomyocyte-derived H9c2 cell line was obtained from the European Collection of Cell Cultures [H9c2 cell line from rat (BDIX heart myoblast), from Sigma-Aldrich (USA)]. Materials for cell culture were obtained from the following sources: the protein assay kit Bio-Rad RC DC was purchased from Bio-Rad Laboratories (USA); all plastic sterile material used in cell culture was obtained from Corning-Costar (USA); phosphate-buffered saline (PBS) and penicillin/streptomycin were obtained from Biochrom (Germany); foetal bovine serum (FBS), Hanks' balanced salt solution, and Dulbecco's phosphate-buffered saline were purchased from Gibco (UK). Other compounds, namely MTX dihydrochloride (MTX, ≥ 97 % purity), peroxidase from horseradish (Type II), trypan blue solution (0.4 %), sodium pyruvate, potassium dihydrogen phosphate, dipotassium hydrogen phosphate, Triton X-100, Dulbecco's modified eagle medium (DMEM)—high glucose, sodium bicarbonate, dimethyl sulphoxide (DMSO), oligomycin, retinoic acid (RA), neutral red (NR) solution, ethanol, trypsin solution, 3-(4,5-dimethylthiazol-2-yl)-2,5-diphenyl tetrazolium bromide (MTT), hydrochloric acid, sodium dodecyl sulphate (SDS), buthionine sulphoximine, β -nicotinamide adenine dinucleotide (NADH), *N*-acetyl cysteine, Ac-Leu-Glu-Thr-Asp-al (Ac-LETD-CHO), caspases 8 and 9 inhibitor, L-carnitine, 3-methyladenine, Hoechst 33258, paraformaldehyde, ethidium bromide, acridine orange, cycloheximide, 3,3'-dihexyloxycarbocyanine iodide (DiO₆), bovine serum albumin, luciferase from *Photinus pyralis* (firefly), D-luciferin sodium salt, glycine sodium salt, tris-base, potassium hydrogen carbonate, and adenosine triphosphate (ATP) were obtained from Sigma-Aldrich (USA). Hydrogen peroxide (H₂O₂) 30 % (Perhydrol®), acetic acid glacial 100 %, ethylenediamine tetra acetic acid (EDTA), and perchloric acid were purchased from Merck (Germany). The solvents used were pro-analysis or high-performance liquid chromatography (HPLC) grade products from Sigma-Aldrich, Chem-Lab NV, Merck, VWR Chemical or Panreac Quimica Sau. Compound purifications were performed by chromatography flash cartridge using silica gel reverse-phase (RP)-18 (Grace Resolv®) and preparative thin-layer chromatography (TLC) using Merck

silica gel HPLC60 RP-18 (GF254) plates purchased from Merck (Germany).

Methods

Synthesis and purification of the mitoxantrone metabolite naphthoquinoxaline

To a solution of MTX dihydrochloride (100 mg, 0.19 mmol) in 16 mL of sodium acetate buffer (pH 6), horseradish peroxidase (HRP) and Perhydrol® (1:1; 20 μ L) were added, and the solution was magnetically stirred for 30 min at room temperature. The reaction was monitored by TLC [methanol/ammonia 0.25 %] and stopped by the addition of diluted hydrochloric acid. After filtration (0.2 μ m, Millipore), the solvent was evaporated under a stream of nitrogen.

The crude product was purified by preparative column chromatography with silica C₁₈ (3 g), using a gradient of methanol:aqueous solution of ammonia 1 % (5:5) until 100 % of methanol alkalized with an aqueous solution of ammonia (25 %). The fractions eluted with methanol:aqueous solution of ammonia 1 % (7:3) containing NAPHT were gathered and the solvent evaporated, furnishing a purple solid. This product was further purified by solid-phase extraction with a cation exchange cartridge Discovery® DSC-SCX, with a sulphonic acid moiety following the steps: elution with methanol (10 mL) followed by solution of methanol/ammonia 1 % (10 mL); the alkaline fractions were collected and the solvent evaporated under reduced pressure to afford a purple solid corresponding to the compound NAPHT. The melting point of the product was obtained in a Köfler microscope. The infrared spectra were obtained in KBr microplate in a Fourier transform infrared spectroscopy spectrometer Nicolet iS10 from Thermo Scientific with Smart OMNI-Transmission accessory (Software OMNIC 8.3) (cm⁻¹). ¹H nuclear magnetic resonance (NMR) spectra were taken in DMSO-d₆ at room temperature, on a Bruker Avance 300 instrument (300.13 MHz for ¹H). Chemical shifts were expressed in δ (ppm) comparatively to tetramethylsilane as an internal reference. Coupling constants were reported in hertz (Hz). Mass spectra were obtained by high-resolution mass spectrometry (HRMS) on a APEX III mass spectrometer, recorded as electrospray ionization mode in Centro de Apoyo Científico e Tecnológico á Investigación (CACTI, University of Vigo, Spain).

HPLC analysis of the synthetic products was performed in a Spectrasystem P4000 Autosampler 3000, Thermo Fisher Scientific™ (USA), equipped with a diode array detector ultraviolet (UV) 8000, and using a C₁₈ column (5 μ m, 150 mm \times 4.6 mm I.D.) from Fortis BIO Technologies (Cheshire, UK). The injected volume was 10 μ L,

and the mobile phase was monitored at 254 nm. ChromQuest™ 5.0 software, version 3.2.1, Thermo Fisher Scientific™ (USA) managed chromatographic data. A linear gradient from 10 to 80 % of eluent B within 30 min (eluent A: 0.1 % aqueous solution of trifluoroacetic acid; eluent B: 100 % methanol) was used at a constant flow rate of 0.5 mL/min. All samples were dissolved in methanol and filtered through a hydrophilic Durapore-GV membrane of 0.45- μm pore size (Millipore) before injection. The retention factor (k) was determined as $[k = (t_R - t_0)/t_0]$, and t_0 was considered to be equal to the peak of the solvent front.

Cell culture experimental protocols

The toxicological evaluation of MTX and NAPHT was carried out in vitro, using differentiated H9c2 cells. H9c2 cells correspond to a cell line isolated from the ventricular part of a thirteenth-day rat heart embryo (Kimes and Brandt 1976). H9c2 cells were maintained in a myoblast proliferative phenotype in the presence of complete medium: DMEM with high glucose supplemented with 10 % FBS and antibiotics (100 units/mL penicillin and 100 $\mu\text{g}/\text{mL}$ streptomycin) at 37 °C with 5 % CO_2 . Cell passaging was done by trypsinization. All experiments were carried out before the cells reached 70–80 % confluence (Ruiz et al. 2012), and the cell line was used between passage 15 and 30.

Differentiation into a “cardiac-like” phenotype was accomplished using culture medium supplemented with 1 % FBS and RA 10 nM (medium changed every 2 days; Pereira et al. 2011; Ruiz et al. 2012). The morphological changes and decreased proliferation rate caused by the differentiation protocol were assessed by phase-contrast microscopy and the fluorescent nuclear dye, Hoechst 33258.

For incubation experiments with MTX or its metabolite, cells were seeded in a density of 24,000 cells/mL. The cells were incubated with the drugs, after the 7-day differentiation protocol described above. MTX was dissolved in PBS; thus, control wells were exposed to the same volume of PBS that was used in the drug wells. NAPHT was dissolved in DMSO, and the maximum concentration *per* well of DMSO used was 0.1 % *v/v*; therefore, the vehicle DMSO was used in control cells in all the experiments performed with NAPHT.

Microscopic evaluation of the cells

Phase-contrast microscopy Cell cultures were assessed morphologically either to confirm differentiation or to evaluate the effect of the drugs by phase-contrast microscopy at selected time-points in a Nikon Eclipse TS100 equipped with a Nikon DS-Fi1 camera (Japan).

Hoechst nuclear staining Hoechst staining was used to assess differentiation and to evaluate the effect of the drugs

on differentiated H9c2 cells. To assess the effect of differentiation in the cellular multiplication, H9c2 cells were seeded in 48-well plates and differentiated or not for 7 days. On the 7th day, cells (differentiated or not) were fixed in 4 % paraformaldehyde (10 min, 4 °C) and washed 3 \times with PBS containing calcium and magnesium. Cells were then stained with the nuclear dye Hoechst 33258 (final concentration 5 $\mu\text{g}/\text{mL}$) for 10 min at 37 °C (protected from light), after which they were washed with PBS containing calcium and magnesium (3 \times) at room temperature. Cells were examined in a Nikon Eclipse TS100 equipped with a Nikon DS-Fi1 camera using a fluorescent filter ($\lambda_{\text{excitation maximum}} = 346 \text{ nm}$ and $\lambda_{\text{emission maximum}} = 460 \text{ nm}$) (Soares et al. 2013). To determine the effect of MTX or NAPHT on nuclear morphology, differentiated cells were incubated with these compounds, and at the end of the incubation period, they were treated as previously described for the Hoechst nuclear staining (Soares et al. 2013).

Ethidium bromide and acridine orange staining The fluorescent DNA-intercalating dyes ethidium bromide and acridine orange are suitable for the microscopic morphological discrimination between necrotic and apoptotic cell death. Ethidium homodimers do not penetrate intact cellular membranes. Therefore, ethidium bromide only intercalates with nucleic acids if the outer cellular membrane is disintegrated. In contrast, the fluorescent cationic dye acridine orange diffuses through intact membranes of live cells and largely accumulates in acidic vesicles (Capela et al. 2013). After the incubation of cells with MTX or NAPHT, the medium was removed and the protocol was done according to what was previously described (Capela et al. 2013). Cells were examined in a Nikon Eclipse TS100 equipped with a Nikon DS-Fi1 camera, using a standard fluorescein filter ($\lambda_{\text{excitation}} = 485 \text{ nm}$ and $\lambda_{\text{emission}} = 525 \text{ nm}$).

Cytotoxicity tests

Lactate dehydrogenase (LDH) kinetic leakage assay After the 24- or 48-h exposure, cell viability was evaluated by measuring membrane integrity. The quantification of LDH activity was made using a spectrophotometric method, based on the reversible reduction of pyruvate to lactate in the presence of β -NADH, as described before (Capela et al. 2006). Cell death was quantified by the percentage of LDH released to the medium over total LDH. Total LDH activity was determined after adding 20 μL of Triton X-100 5 % to each well followed by a 30-min incubation at 37 °C.

Viability assays with caspases 8 and 9 inhibitor, Ac-LETD-CHO (200 and 100 μM ; Shi and Shen 2008), the antioxidant *N*-acetyl cysteine (1 mM; glutathione precursor and reactive species scavenger; Martins et al. 2013; Rossato et al. 2013b), buthionine sulphoximine (50 μM ; inhibitor of gamma-glutamylcysteine synthetase; Ferreira et al. 2013),

L-carnitine (2 mg/mL; mitochondrial enhancer that acts as a carrier for fatty acids across the inner mitochondrial membrane for subsequent β -oxidation; Rossato et al. 2013b), 3-methyladenine (2.5 mM; autophagy inhibitor; Soares et al. 2014) were performed. These compounds were added 1 h prior to cells' exposure to MTX 2 μ M. For NAPHT experiments with *N*-acetyl cysteine (1 mM), this later compound was added 1 h prior to the addition of NAPHT 2 μ M.

MTT reduction assay The MTT assay was done to evaluate the cytotoxicity of MTX and NAPHT in differentiated H9c2 cells. This colorimetric assay relies mostly on the ability of mitochondrial complexes (or other dehydrogenases) to convert the soluble yellow tetrazolium dye, MTT, into an insoluble blue formazan product that can be measured at 550 nm (Costa et al. 2009b). After the incubation period, culture media was removed and the protocol was done according to what was previously described (Capela et al. 2006), with cells being incubated at 37 °C for 4 h with MTT (final concentration 500 μ g/mL). The percentage of MTT reduction of control/vehicle cells was set to 100 %, and the effects resulting from the incubation with MTX or metabolite were expressed as the percentage to the respective control or vehicle cells. The MTT test was also done to evaluate the effect of cycloheximide (10 μ g/mL), a glutarimide antibiotic that blocks the translation of messenger RNA on cytosolic, 80S ribosomes, but does not inhibit organelle protein synthesis (Gupta et al. 2006), and oligomycin (5 μ M), an inhibitor of mitochondrial ATP synthase (Rossato et al. 2013b) towards MTX cytotoxicity. Cycloheximide and oligomycin were added 30 min before MTX.

Neutral red (NR) lysosomal uptake assay The amount of NR dye incorporated into the cells represents their lysosomal functionality, as this dye easily penetrates viable cell membranes and accumulates in lysosomes (Soares et al. 2013). At the end of the incubation time, the amount of NR cellular uptake was determined as previously described by us (Soares et al. 2013). Absorbance was measured at 540 nm, in a 48-well plate reader [Biotech Synergy HT (VT, USA)], and results were compared to control/vehicle wells whose mean values were set to 100 % (Soares et al. 2013).

Moreover, the NR test was done to access the effects of 3-methyladenine (2.5 mM) and oligomycin (5 μ M) on cells before the exposure to MTX (and also 3-methyladenine in the case of NAPHT) in differentiated H9c2 cells. 3-Methyladenine was added 1 h before MTX (or NAPHT), while oligomycin was added 30 min before MTX.

Evaluation of mitochondrial potential

The evaluation of the mitochondrial potential was done according to Freitas et al. (2013), with some modifications.

Briefly, after the 7-day differentiation protocol, cells were incubated for 12 h with MTX or NAPHT and subsequently incubated for 30 min at 37 °C with DiO₆ (35 nM/well). Also, a well in each condition was tested without any DiO₆ to evaluate whether any component of the medium or drugs tested had any residual fluorescence that could interfere with the readings being done. After the 30-min incubation time, the cells were washed twice with warm PBS with calcium and magnesium. Photographs were taken in a fluorescent microscope (Nikon Eclipse TS100 equipped with a Nikon DS-Fi1 camera) with the standard fluorescein filter ($\lambda_{\text{excitation}} = 485$ nm and $\lambda_{\text{emission}} = 520$ nm), and fluorescence was quantified in a plate reader (BioTek Instruments, Powerwave X, USA). The results were expressed as arbitrary fluorescence units (FUs).

Determination of cellular ATP levels

For this assay, H9c2 cells were seeded in 6-well plates. The ATP levels were evaluated in differentiated H9c2 cells incubated for 24 h with 2 and 5 μ M of MTX or NAPHT. Moreover, the ATP levels were assessed following MTX incubation for 24 h, with a 30-min pre-incubation with oligomycin.

Subsequently to the incubation period, the medium was discarded and cells were washed with cold PBS with calcium and magnesium (750 μ L/well). Cells were then scrapped with new cold PBS containing calcium and magnesium, and 2 wells per each condition were gathered. Cells were centrifuged at 5,000 rpm, 4 °C, for 10 min, and the supernatant was rejected. Two hundred μ L of cold 5 % perchloric acid was added to the pellet, vortexed, and centrifuged at 13,000 rpm, for 10 min, at 4 °C. The acidic supernatant obtained was collected for ATP determination and placed at -80 °C. The pellet was stored at -20 °C and used for protein evaluation. ATP levels were assessed by a bioluminescence reaction with the firefly luciferin–luciferase system, as previously described (Costa et al. 2007). The levels of ATP were expressed as nmol of ATP per amount of protein or as % of control after protein normalization.

Determination of glucose, lactate and alanine levels in H9c2 cells medium

The levels of glucose and lactate were determined by proton nuclear magnetic resonance (¹H NMR) in the cellular medium after MTX and NAPHT incubation for 24 and 48 h. The medium of control/vehicle, MTX and NAPHT-incubated cells was removed and immediately frozen. Each NMR sample consisted of 160 μ L of supernatant and 40 μ L of 2 mM sodium fumarate solution in D₂O, used as an internal standard. ¹H NMR spectra were

acquired in a 600 MHz Varian Spectrometer equipped with a 3-mm inverse detection NMR probe. Spectrum acquisition parameters included a 30° radiofrequency excitation pulse, a 3-s acquisition time (24 k points covering a sweep width of 8 kHz), and a pre-acquisition delay of 7 s, which included a 3-s water saturation delay, for allowing complete nuclei relaxation for quantification purposes. Each spectrum consisted of a total of 32 accumulations to achieve adequate signal to noise. A 0.2-Hz exponential multiplication function and zero filling were applied to the free induction decay (FID) before Fourier transformation using the NutsPro™ (AcornNMR Inc., Fremont, USA). Energetic metabolite concentration was made by spectral deconvolution of the glucose-H1 α (doublet at $\delta = 5.22$ ppm), and lactate-CH₃ (doublet at $\delta = 1.33$ ppm) resonances and subsequent comparison with the fumarate resonance (singlet $\delta = 6.50$ ppm).

Protein determination

Protein content was determined by the Bio-Rad RC DC protein assay kit, according to the manufacturer's instructions.

Statistical analysis

The data are presented as mean \pm standard deviation (SD) of different independent experiments. Statistical analyses were carried out by the nonparametric ANOVA (Kruskal–Wallis test) followed by the Dunn's post hoc test once a significant p was achieved. When the distribution was normal, one-way ANOVA was performed followed by the Tukey's post hoc test. Statistical significance was considered with p values <0.05 . All statistical analysis was done using the GraphPad Prism 6 software program (USA).

Results

Synthesis and structure determination of the mitoxantrone metabolite naphthoquinoline

The synthesis of the MTX metabolite was accomplished through the HPR-catalysed H₂O₂ oxidation of MTX, and the major product isolated from this reaction is depicted in Fig. 1a. With the enzymatic oxidation of MTX, several derivatives could be observed by chromatographic analysis; however, the purified derivative isolated and identified was NAPHT, already proposed as a two-electron oxidized product of the peroxidase-catalysed H₂O₂ oxidation of MTX (Bruck and Bruck 2011; Fig. 1b). First attempts to purify the crude product using normal-phase chromatography were unsuccessful due to the retention of MTX derivatives in the stationary

phase. Thus, procedures involving reverse-phase and/or ion exchange chromatography that have shown great versatility and ability for retaining and separating a variety of charged polar compounds were used for the isolation of NAPHT (See "Methods" section).

Analysis of the reaction mixture by HPLC indicated that the majority of MTX reacted after 30 min. The calculated HPLC yield for the product NAPHT (considering their areas as MTX) was 85 %, while the precursor MTX, at that time-point, represented 2 % of the total product (Fig. 2a). MTX and NAPHT show similar spectral features between 200 and 300 nm, but slight differences were observed in the visible range (Fig. 2b, c, respectively). MTX shows absorbance maxima at 609 and 660 nm as previously reported (Bruck and Harvey 2003); NAPHT revealed absorbance maxima at 584, 633 nm and a shoulder at 550 nm, which was previously described for this two-electron oxidized metabolite (Kolodziejczyk et al. 1988; Reszka and Chignell 1996).

The structural elucidation of NAPHT was established by HRMS, infrared, and by NMR techniques. The HRMS-ESI gave for NAPHT the accurate molecular mass of 442.18469 and the molecular formula C₂₂H₂₆N₄O₆. These data suggested that the isolated compound NAPHT corresponded to 8,11-dihydroxy-4-(2-hydroxyethyl)-6-[[2-[(2-hydroxyethyl)-amino]-ethyl]-amino]-1,2,3,4,7,12-hexahydronaphtho-[2,3-*f*]-quinoxaline-7,12-dione. The following data were obtained: NAPHT, 97 % purity by HPLC-diode array detector; melting point 112–115 °C (methanol); infrared spectroscopy (KBr) ν_{\max} : 3443, 2925, 1631, 1602, 1560, 1541, 1458, 1385, 1340, 1248; and HRMS (ESI⁺) m/z calculated for C₂₂H₂₆N₄O₆: 442.1852, found: 442.18469. The ¹H NMR data (DMSO-*d*₆, 300.13 MHz) of MTX and NAPHT are presented in Table 1. The multiplicity and coupling constants of the protons observed in the ¹H NMR spectrum of MTX showed the existence of two symmetrical 1,4-disubstituted aromatic rings, the signals of the protons of the hydroxyl and amine groups and of the aliphatic chains. In turn, the ¹H NMR spectrum of NAPHT showed a different pattern for substitution in one of the aromatic rings, while the proton signals of methylene groups, characteristic of the linear aliphatic lateral chain, were maintained. The presence of the piperazine ring with C-5/C-6 of the aromatic ring of the anthraquinone is evidenced by the lack of H-6 signal and the presence of a singlet corresponding to H-7 and of two aromatic protons, corresponding to H-2 and H-3 (for numbering of structures see Table 1).

Differentiation decreased cell division and changed morphological characteristics of H9c2 cells

The differentiation protocol was conducted with medium supplemented with 1 % FBS and 10 nM RA for 7 days. Cells came to resemble the cardiac phenotype after the

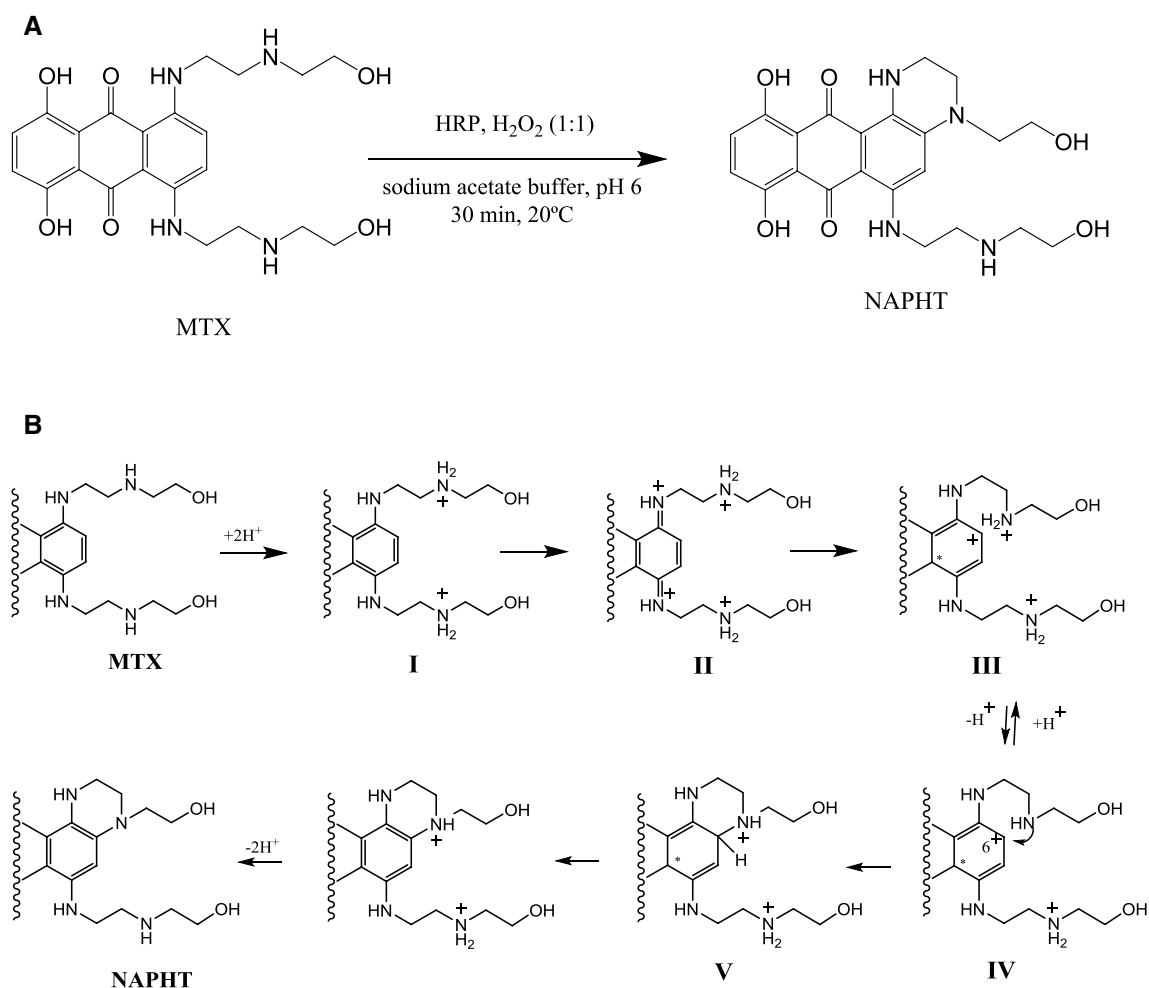


Fig. 1 **a** Isolated product of the incubation of MTX with horseradish peroxidase (HRP) was NAPHT. **b** Proposed mechanism for the formation of NAPHT after the oxidation of MTX. The proposed mechanism for the formation of NAPHT establishes the reaction to proceed via a two-electron oxidation of the phenylenediamine substructure I

to the formation of the highly reactive quinone II. The non-protonated form IV of the equilibrium reacts by an intramolecular attack of the basic amino group of the side chain with the electrophilic centre at C-6 of MTX radical cation III. Subsequent oxidation of the cyclized radical V led to the formation of NAPHT

7-day differentiation protocol: cell division was dramatically reduced, while the cellular density was substantially higher in undifferentiated cells cultivated for 7 days with 10 % FBS medium without RA, as verified by the Hoechst 33258 staining and morphological evaluation (data not shown). Also, the cell bodies of differentiated cells became smaller and fusiform when compared to undifferentiated cells that exhibit a large and flat cell body. Overall, differentiated cells established a more organized network bearing a more cardiac-like morphology, as shown by phase-contrast morphology (Fig. 3a).

Mitoxantrone causes higher cellular damage in differentiated H9c2 cells than does its naphthoquinoxaline metabolite

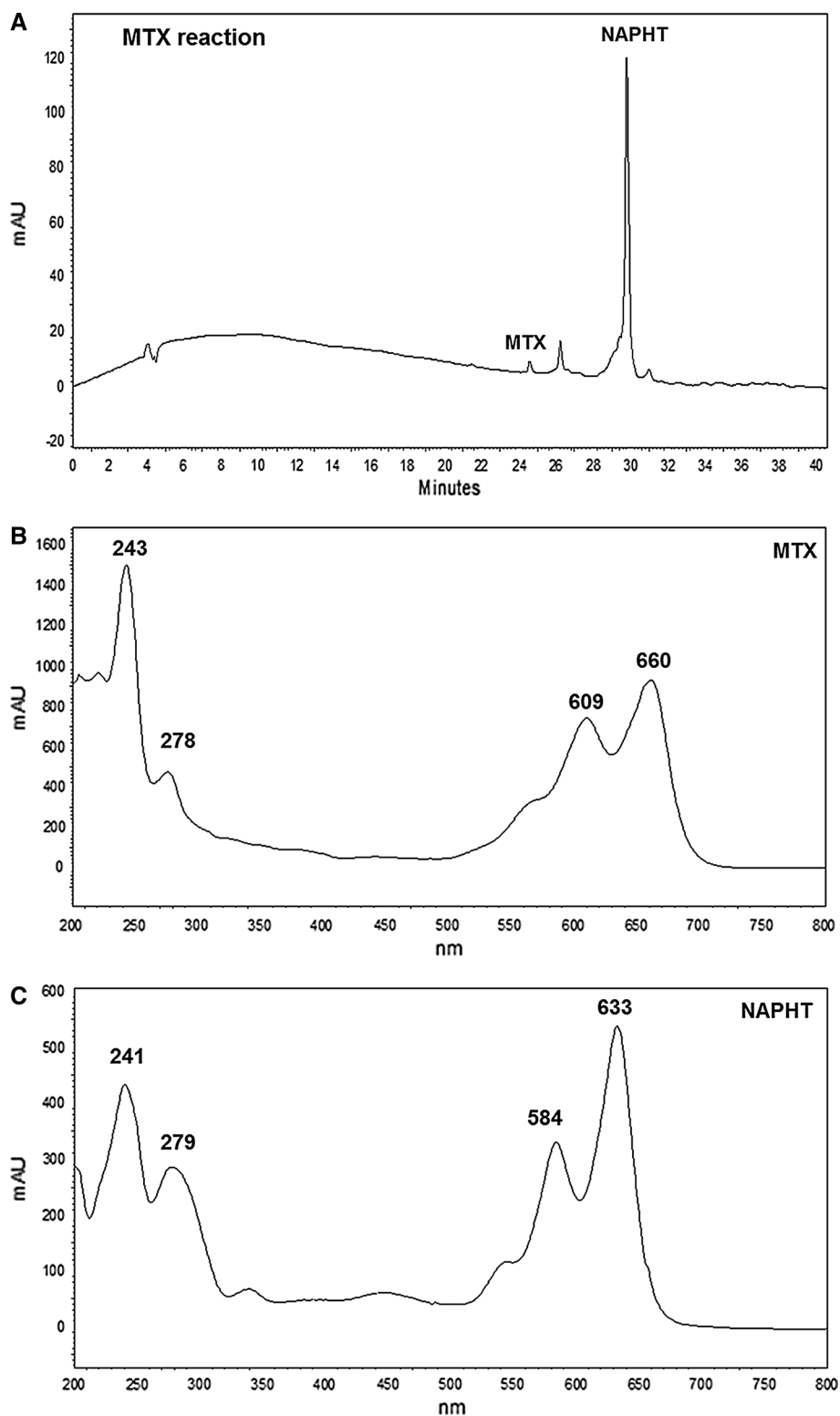
H9c2 cells were incubated with MTX (2 or 5 μ M), as described in Methods section (Fig. 3a–c). After a 24-h

incubation, phase-contrast microscopy revealed cell death, with intensifying features of cell death with increasing MTX concentration (Fig. 3b, c). In particular, H9c2 cells exposed to 5 μ M of MTX showed signs of membrane integrity loss and substantial decreases in cell number (Fig. 3c). No significant signs of nuclear alteration were found by Hoechst staining at 24 h, when compared to control (Fig. 3d–f).

Ethidium bromide/acridine orange staining was also used: living cells appear with a regular-sized green fluorescent nucleus, as shown in control H9c2 cells in Fig. 3g. The number of cells largely decreased with increased MTX concentration, but cells present in the field maintained a green nucleus, although with evident cytoplasmic injury (Fig. 3h, i).

At 48 h, the cell injury was progressively higher in MTX-incubated cells as observed in all photographs and stainings performed (data not shown).

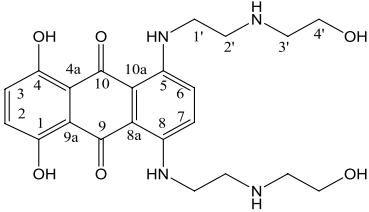
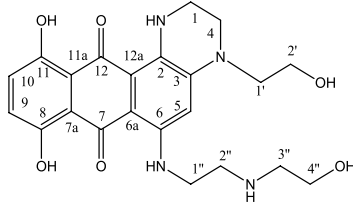
Fig. 2 Representative HPLC chromatograms [$\lambda = 254$ nm, in a C_{18} column, linear gradient from 10 to 80 % of eluent B within 30 min (eluent A: 0.1 % aqueous solution of trifluoroacetic acid; eluent B: 100 % methanol)] of 6.63 mg/mL solution of the crude product [MTX ($k = 5.1$) and NAPHT ($k = 6.3$)] (a). UV spectra of MTX (b) and of the isolated product, NAPHT (c)



H9c2 cells were also incubated with NAPHT (2 or 5 μ M). Phase-contrast microscopy, after a 24-h incubation, revealed concentration-dependent cell injury (Fig. 4b, c). A decrease in cell number was observed (Fig. 4b, c), although lower than observed for MTX. No

apoptotic nuclei were observed (Fig. 4e, f) after Hoechst staining. At 48 h, the cell injury increased in the NAPHT-incubated cells (data not shown), but it was still lower than observed in MTX-incubated cells in the same incubation time.

Table 1 ^1H NMR data of MTX and NAPHT

 MTX		 NAPHT	
1-OH	13.44, <i>s</i> , 2H	8-OH	14.36, <i>s</i> , 1H
4-OH		11-OH	13.56, <i>s</i> , 1H
5-NH	10.41, <i>brs</i> , 2H	2-NH	10.95, <i>s</i> , 1H
8-NH		6-NH	11.34, <i>s</i> , 1H
H-2	7.65, <i>s</i> , 2H	H-9	7.00–6.97, <i>m</i> , 2H
H-3		H-10	
H-6	7.19, <i>s</i> , 2H	H-5	6.19, <i>s</i> , 1H
H-7			
4'-OH	5.34, <i>brs</i> , 2H	4''-OH	4.96, <i>s</i> , 1H
4''-OH	5.34, <i>brs</i> , 2H	2'-OH	4.66, <i>s</i> , 1H
H-1'	3.89–3.87, <i>m</i> , 2H	H-1''	3.72, <i>m</i> , 4H
H-1''		H-1	
H-2'	3.69–3.66, <i>m</i> , 4H	H-2''	3.63, <i>m</i> , 4H
H-2''		H-4	
H-3'		H-3''	2.89, <i>t</i> , 4H
H-3''		H-1'	
H-4'	3.07–3.05, <i>m</i> , 2H	H-2'	2.69, <i>t</i> , 4H
H-4''		H-4''	

Values in ppm (δ_{H}) relative to Me_4Si as an internal reference. *J* values are in Hz
s Singlet, *t* triplet, *m* multiplet

Ethidium bromide/acridine orange staining was also used to evaluate NAPHT effects on H9c2 cells. Vehicle-incubated H9c2 cells showed regular-sized green fluorescent nucleus (Fig. 4g). The NAPHT-incubated (2 or 5 μM) cells show green nucleus, although with signs of cytoplasmic injury (Fig. 4h, i).

Mitoxantrone and its metabolite produce time- and concentration-dependent mitochondrial dysfunction in differentiated H9c2 cells, although less pronounced in the metabolite

The MTT reduction test was done at 2 time-points (24 and 48 h) using several MTX concentrations (0.01–5 μM). At 24 h, MTX (0.1 μM) already caused significant cytotoxicity when compared to control cells (Fig. 5a). At 48 h, as can be seen in Fig. 5b, the MTX-elicited cytotoxicity was even higher, when compared to control and to the same concentrations in the earlier time-point evaluated. Similar results were seen with other concentrations, with a time-dependent

increase in cytotoxicity. The 0.01 μM concentration showed no cytotoxicity when compared to control at both time-points evaluated.

The ability of NAPHT to interfere with MTT reduction was also evaluated at 2 time-points (24 and 48 h) using several NAPHT concentrations (1–5 μM). At 24 h, 2 and 5 μM of NAPHT caused cytotoxicity when compared to vehicle, whereas 1 μM NAPHT did not cause significant cytotoxicity (Fig. 6a). At 48 h, NAPHT caused even higher cytotoxicity (Fig. 6b). The vehicle (DMSO 0.1 % *v/v*) did not cause any significant change when compared to control cells.

Mitoxantrone caused a greater loss of cellular membrane integrity than did its naphthoquinoline metabolite

The ability of MTX to cause cell membrane disruption was tested by measuring LDH in the extracellular medium at 2 time-points (24 and 48 h) using several concentrations

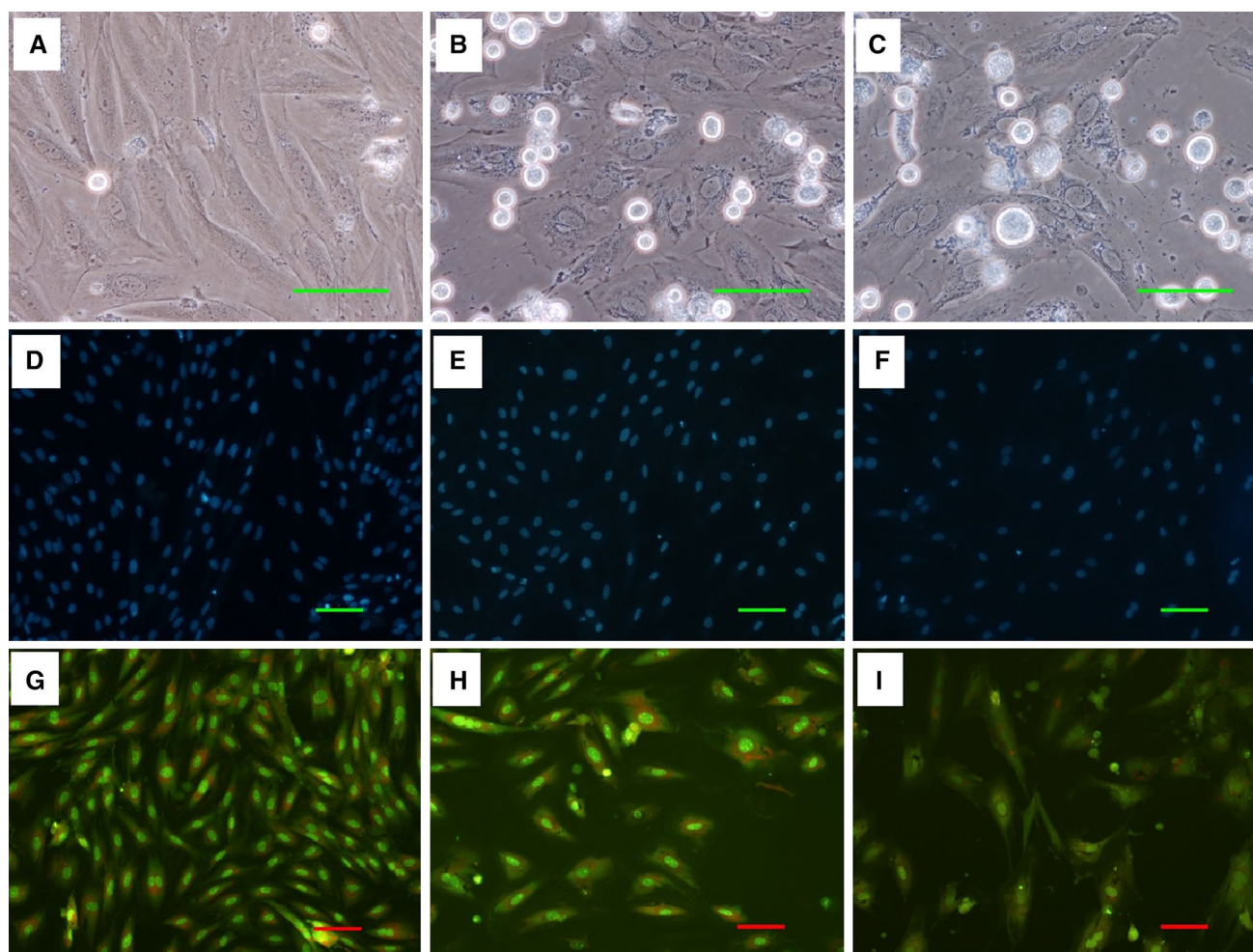


Fig. 3 Phase-contrast microphotographs (a–c), Hoechst 33258 (d–f) and ethidium bromide and acridine orange (g–i) stainings. Phase-contrast microscopy of control (a), MTX 2 μ M (b), MTX 5 μ M (c) differentiated H9c2 cells incubated for 24 h. Fluorescence microscopy (Hoechst 33258 staining) of control (d), MTX 2 μ M (e), MTX

5 μ M (f) differentiated H9c2 cells incubated for 24 h. Fluorescence microscopy (ethidium bromide and acridine orange) of control (g), MTX 2 μ M (h), MTX 5 μ M (i) differentiated H9c2 cells incubated for 24 h. Images are representative of three independent experiments (scale bar represents 100 μ m)

(0.01–5 μ M). At 24 h, only the three highest concentrations of MTX (1, 2 and 5 μ M) caused significant loss of cellular membrane integrity when compared to control cells (Fig. 5c). At 48 h, MTX caused a higher cellular toxicity (Fig. 5d). The other concentrations showed no significant cytotoxicity in this test.

The ability of NAPHT to cause cell death was also tested at 2 time-points (24 and 48 h) and with several concentrations (1–5 μ M). At 24 h, all the concentrations of NAPHT (1, 2 and 5 μ M) tested caused significant cellular membrane integrity loss when compared to vehicle cells (Fig. 6c). After 48 h, NAPHT caused a significant decrease in cellular integrity (Fig. 6d). The vehicle (DMSO 0.1 % v/v) did not cause any significant change in viability when compared to control cells.

Mitoxantrone caused a higher lysosome uptake dysfunction in differentiated H9c2 cells than does its metabolite

The lysosomal uptake of NR was evaluated after MTX incubation at two time-points. The highest concentrations of MTX (1, 2 and 5 μ M) caused a substantial impairment of lysosomal uptake of NR when compared to control cells. That cytotoxicity was concentration- and time-dependent (Fig. 5e, f).

Lysosomal uptake of NR was evaluated after 24-h or exposure to several concentrations of NAPHT (1–5 μ M). At 24 h, the two highest concentrations of NAPHT (2 and 5 μ M) substantially impaired lysosomal uptake of NR when compared to vehicle-incubated cells (Fig. 6e) and

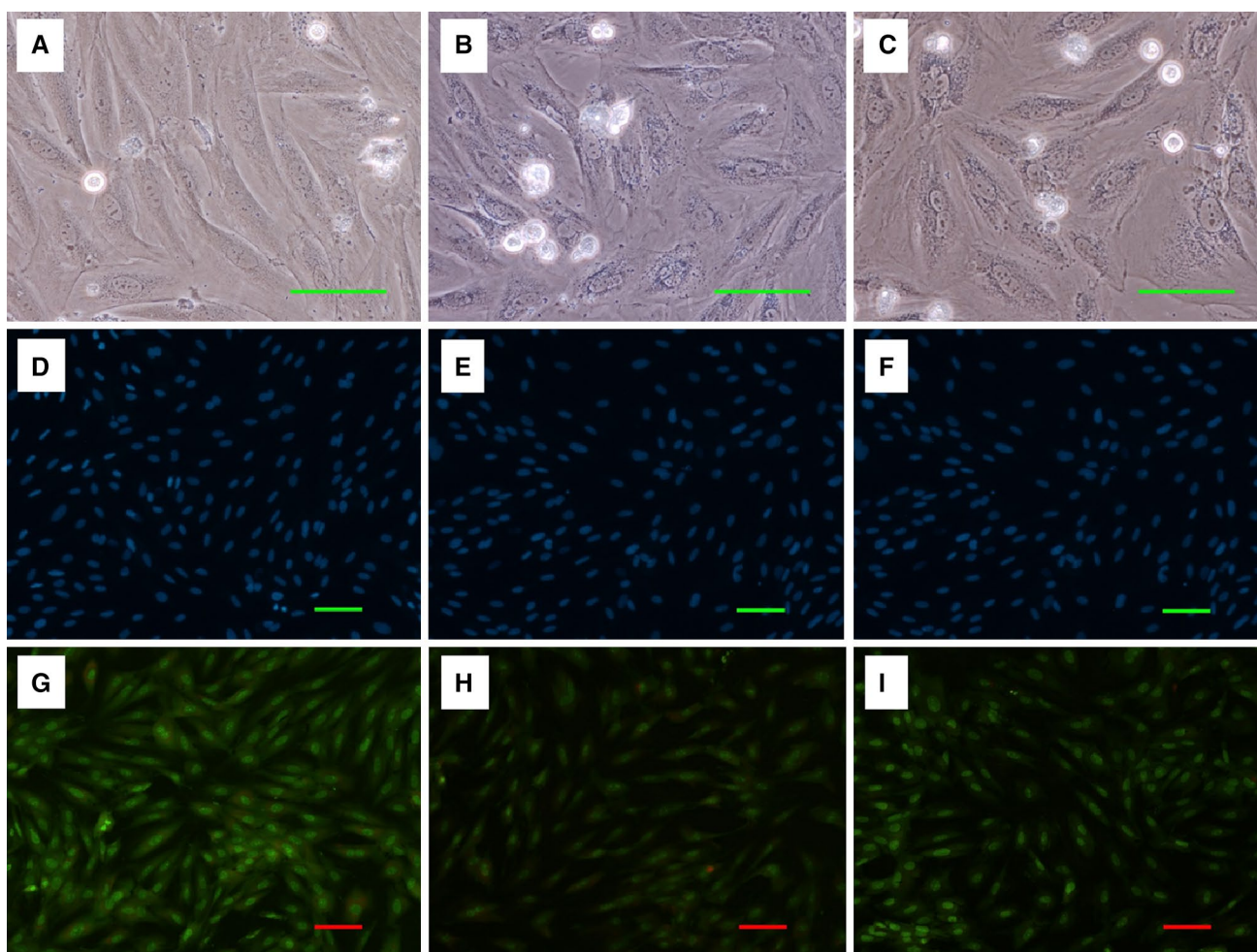


Fig. 4 Phase-contrast microphotographs (a–c), Hoechst 33258 (d–f) and ethidium bromide and acridine orange (g–i) stainings. Phase-contrast microscopy of vehicle (a), NAPHT 2 μM (b), NAPHT 5 μM (c) in differentiated H9c2 cells incubated for 24 h. Fluorescence microscopy (Hoechst 33258 staining) of vehicle (d), NAPHT 2 μM (e), NAPHT 5 μM (f) in differentiated H9c2 cells incubated for 24 h.

Fluorescence microscopy (ethidium bromide and acridine orange) of vehicle (g), NAPHT 2 μM (h), NAPHT 5 μM (i) in differentiated H9c2 cells incubated for 24 h. DMSO (final concentration of 0.1 % v/v) was used as vehicle. Images are representative of three independent experiments (scale bar represents 100 μm)

that cytotoxicity was further increased after a 48-h incubation (Fig. 6f). The vehicle (DMSO 0.1 % v/v) did not cause any significant change in this parameter, when compared to control cells.

Mitoxantrone and its naphthoquinoline metabolite caused concentration-dependent early mitochondrial dysfunction

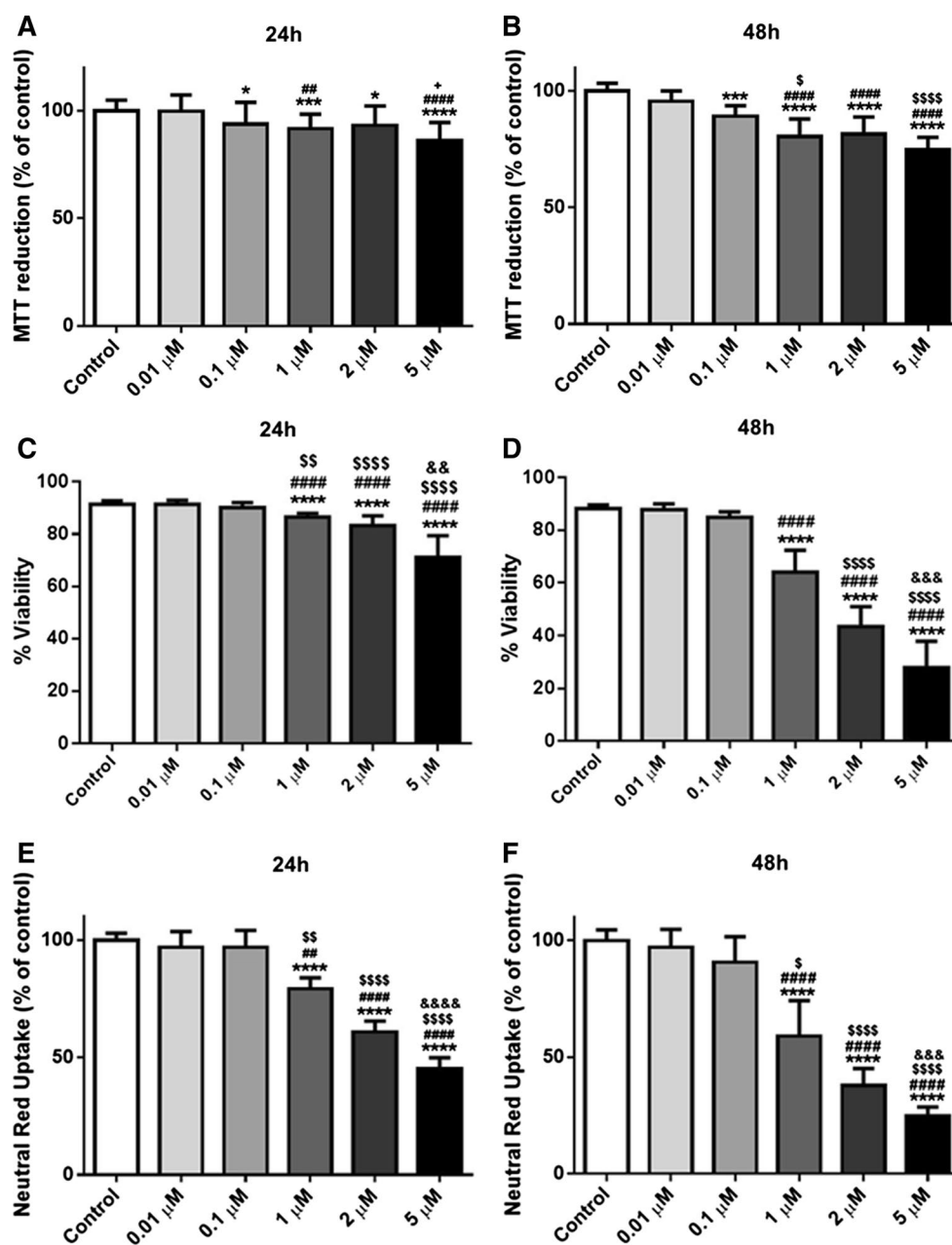
Assessment of mitochondrial membrane potential in differentiated H9c2 cells incubated with MTX or NAPHT for 12 h was performed. Lower levels of fluorescence were observed after MTX treatment when compared to control cells, suggesting that depolarization of mitochondrial membrane potential occurred. This depolarization was concentration dependent (Fig. 7d). NAPHT also caused significant

dose-dependent decreases in mitochondrial membrane potential after a 12-h incubation (Fig. 7h).

Mitoxantrone significantly increased intracellular ATP levels and lactate levels in H9c2 cells media in a concentration-independent manner, whereas its metabolite did not significantly change those parameters

To understand whether MTX elicited any effects in cellular energetic parameters, intracellular ATP levels, cellular glucose and lactate levels in the media were determined in H9c2 cells exposed to MTX or NAPHT. At 24 h, MTX increased the ATP levels (Fig. 8a), the intracellular ATP levels being about 41.10 ± 5.65 nmol/mg protein in 2 μM MTX and 44.63 ± 8.80 nmol/mg

Fig. 5 Mitochondrial dysfunction evaluated by MTT reduction assay (a, b), cellular viability evaluated using the LDH leakage assay (c, d) (% of extracellular LDH/total LDH), and the NR uptake assay (e, f) in differentiated H9c2 cells incubated with 0.01, 0.1, 1, 2 and 5 μM of MTX for 24 (a, c, e) and 48 h (b, d, f). Results are presented as mean \pm SD of five independent experiments (total of 30 wells). Statistical analyses were performed using the Kruskal–Wallis test, followed by the Dunn's post hoc test (* $p < 0.05$; *** $p < 0.001$; **** $p < 0.0001$ vs. control; ## $p < 0.01$; #### $p < 0.0001$ vs. 0.01 μM ; § $p < 0.05$; §§ $p < 0.01$; §§§ $p < 0.0001$ vs. 0.1 μM ; && $p < 0.01$; &&& $p < 0.001$; &&&& $p < 0.0001$ vs. 1 μM ; + $p < 0.05$ vs. 2 μM)



protein in 5 μM MTX-incubated cells when compared to 16.87 ± 1.54 nmol/mg protein for the control group. At 24 h, the levels of glucose on the cellular medium did not change after MTX exposure (Fig. 8c). However, MTX significantly changed the lactate levels in the cellular medium as can be seen in Fig. 8e. At 48 h, the glucose levels did not change with MTX treatment, while the levels of lactate were still significantly lower after MTX incubation when compared to control cells (data not shown).

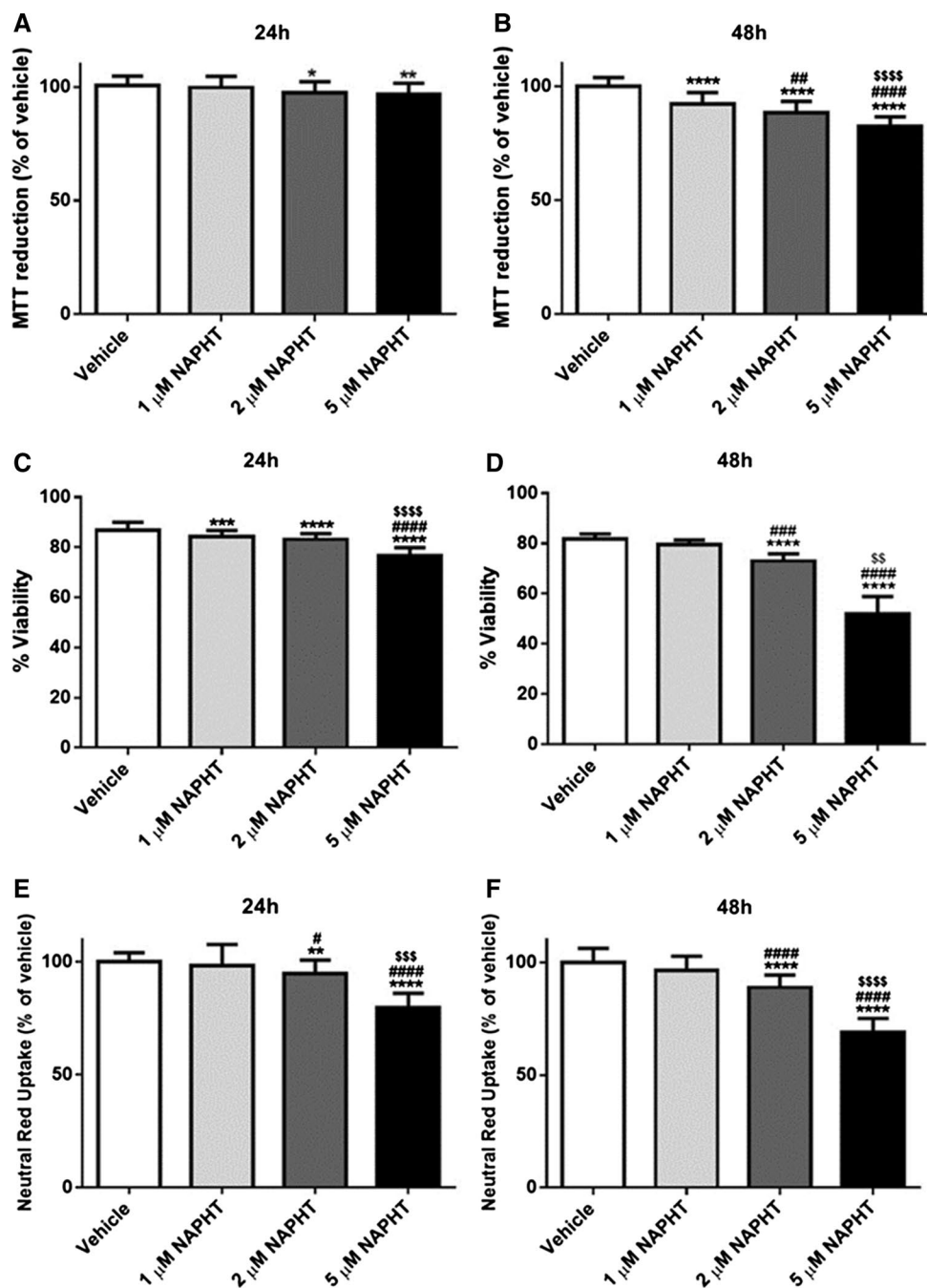
To study whether NAPHT had any effect on cellular energetic, several parameters were assessed in H9c2 cells exposed to NAPHT for 24 h, namely intracellular ATP, and glucose and lactate levels in the cellular medium. At the

NAPHT concentrations (2 and 5 μM) and in the 24 h time-point, no changes were detected in any of the mentioned parameters (Fig. 8b, d, f). Furthermore, at 48 h the medium glucose or lactate levels did not change after NAPHT incubation (data not shown).

Oligomycin exacerbated MTX-induced cytotoxicity and prevented the increase in ATP in MTX-incubated cells

Acknowledging the increase in intracellular ATP levels after MTX exposure and the fact that oligomycin interferes mostly with the mitochondrial complex V (ATP synthase),

Fig. 6 Mitochondrial dysfunction evaluated by MTT reduction assay (a, b), cellular viability evaluated using the LDH leakage assay (c, d) (% of extra-cellular LDH/total LDH), and NR uptake assay (e, f) (% of vehicle) in differentiated H9c2 cells incubated with 1, 2 and 5 μM of NAPHT for 24 h (a, c, e) and 48 h (b, d, f). Results are mean \pm SD of five independent experiments (30 wells) (e, f) or 6 independent experiments (35–36 wells) (a–d). Statistical analyses performed: (d, e) Kruskal–Wallis test, followed by the Dunn’s post hoc test or (a, b, c, f) ANOVA test, followed by the Tukey’s post hoc test (* $p < 0.05$; ** $p < 0.01$; *** $p < 0.001$; **** $p < 0.0001$ vs. vehicle; # $p < 0.05$; ## $p < 0.01$; ### $p < 0.001$; #### $p < 0.0001$ vs. 1 μM ; \$\$ $p < 0.01$; \$\$\$ $p < 0.001$; \$\$\$\$ $p < 0.0001$ vs. 2 μM). DMSO (final concentration of 0.1 % v/v) was used as vehicle



the effect of oligomycin on MTX-induced cytotoxicity after a 24-h incubation was assessed. In the MTT reduction assay, the incubation of cells with oligomycin alone most likely led to a compensatory effect on complexes I and II; therefore, oligomycin per se had similar values (98.36 ± 11.91 %) to control (100.00 ± 5.05 %). However, when cells were pre-incubated with oligomycin, the cytotoxicity caused by MTX largely increased as seen in Fig. 9a. The NR uptake test showed similar results, since oligomycin 5 μM significantly increased the cytotoxicity of either the lower (2 μM) and the highest (5 μM) MTX concentrations tested (Fig. 9b) after a

24-h incubation. However, in this cytotoxicity test, oligomycin per se decreased NR uptake ability of H9c2 cells, resulting in values of 33.82 ± 11.89 % when compared to control values of 100 ± 12.23 %.

To assess whether ATP synthase activity was involved in the increase in ATP levels caused by MTX, H9c2 cells were pre-incubated with oligomycin (Fig. 9c) and compared to control levels of ATP (100 ± 51.66 %). It was clear that the increase of 443.7 ± 95.45 % caused by exposure to 5 μM MTX for 24 h was significantly lower in 5 μM MTX + oligomycin-incubated cells (43.21 ± 59.23 %) (Fig. 9c).

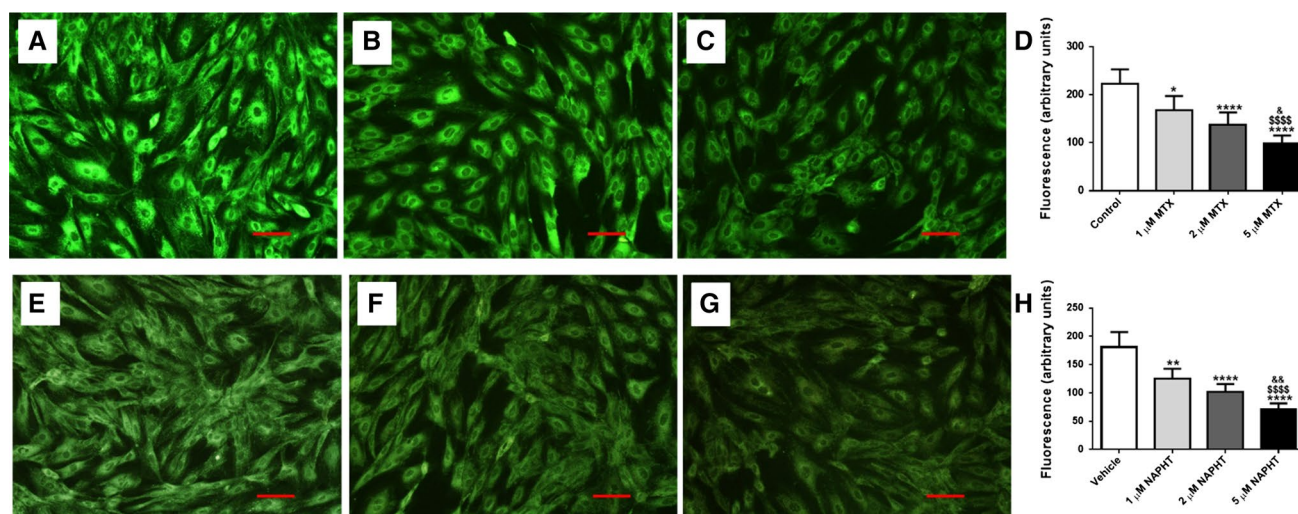


Fig. 7 Images of mitochondrial transmembrane potential of control cells (a), 2 (b) and 5 (c) μM MTX-incubated differentiated H9c2 cells for 12 h and images of mitochondrial transmembrane potential of vehicle cells (e) and differentiated H9c2 cells after incubation with 2 (f) and 5 (g) μM NAPHT for 12 h. Images are representative of three independent experiments (scale bar represents 100 μm). Results of fluorescence (arbitrary units) in differentiated H9c2 cells incubated with 1, 2, and 5 μM of MTX (d) or 1, 2, and 5 μM of NAPHT (h)

3-Methyladenine, an autophagy inhibitor, partially protected against lysosomal uptake dysfunction caused by mitoxantrone and naphthoquinoxaline

3-Methyladenine is used to inhibit and study the mechanism of autophagy (lysosomal self-degradation) and cell death. At 24 h, 3-methyladenine was able to partially prevent the cytotoxicity caused by 2 μM MTX, through the NR uptake assay (data not shown). At 48 h, 3-methyladenine also protected against MTX-induced cytotoxicity, as can be seen in Fig. 10a. However, in the LDH leakage assay, 3-methyladenine was not able to counteract the 2 μM MTX-induced cell death at 48 h (data not shown). The use of 3-methyladenine at 2.5 mM per se did not cause any toxicity when compared to control cells at either time-point evaluated or cytotoxicity test performed.

Other pharmacologically active molecules were also tested to determine possible mechanisms of MTX cytotoxicity. Cells were pre-incubated with buthionine sulphoximine (50 μM), an inhibitor of gamma-glutamylcysteine synthetase, or *N*-acetyl cysteine (1 mM), a glutathione precursor and reactive species scavenger, to access whether the glutathione intracellular values would alter the cytotoxicity caused by MTX. Neither buthionine sulphoximine nor *N*-acetyl cysteine attenuated the cell death elicited by the 48-h incubation of 2 μM MTX (data not shown). Also, neither *L*-carnitine (2 mg/mL), a carrier for fatty acids across the inner mitochondrial membrane, nor the caspase

for 12 h are presented as mean \pm SD of five independent experiments (total of 22 wells) for MTX or six independent experiments (total of 28 wells) for NAPHT. Statistical analyses were performed using the Kruskal–Wallis test, followed by the Dunn’s post hoc test (* $p < 0.05$; ** $p < 0.01$; **** $p < 0.0001$ vs. control/vehicle; SSSS $p < 0.0001$ vs. 1 μM ; & $p < 0.05$; && $p < 0.01$ vs. 2 μM). DMSO (final concentration of 0.1 % v/v) was used as vehicle for NAPHT-exposed cells

inhibitor (100 or 200 μM) afforded any significant protection regarding the 48-h exposure to 2 μM MTX (data not shown). Moreover, cycloheximide (10 $\mu\text{g/mL}$), a protein synthesis inhibitor, also did not prevent the MTX-induced cytotoxicity in H9c2 cells at 48 h in the MTT reduction assay (data not shown).

The pre-incubation with *N*-acetyl cysteine increased cell death caused by naphthoquinoxaline, whereas 3-methyladenine partially protected H9c2 cells against its induced cytotoxicity

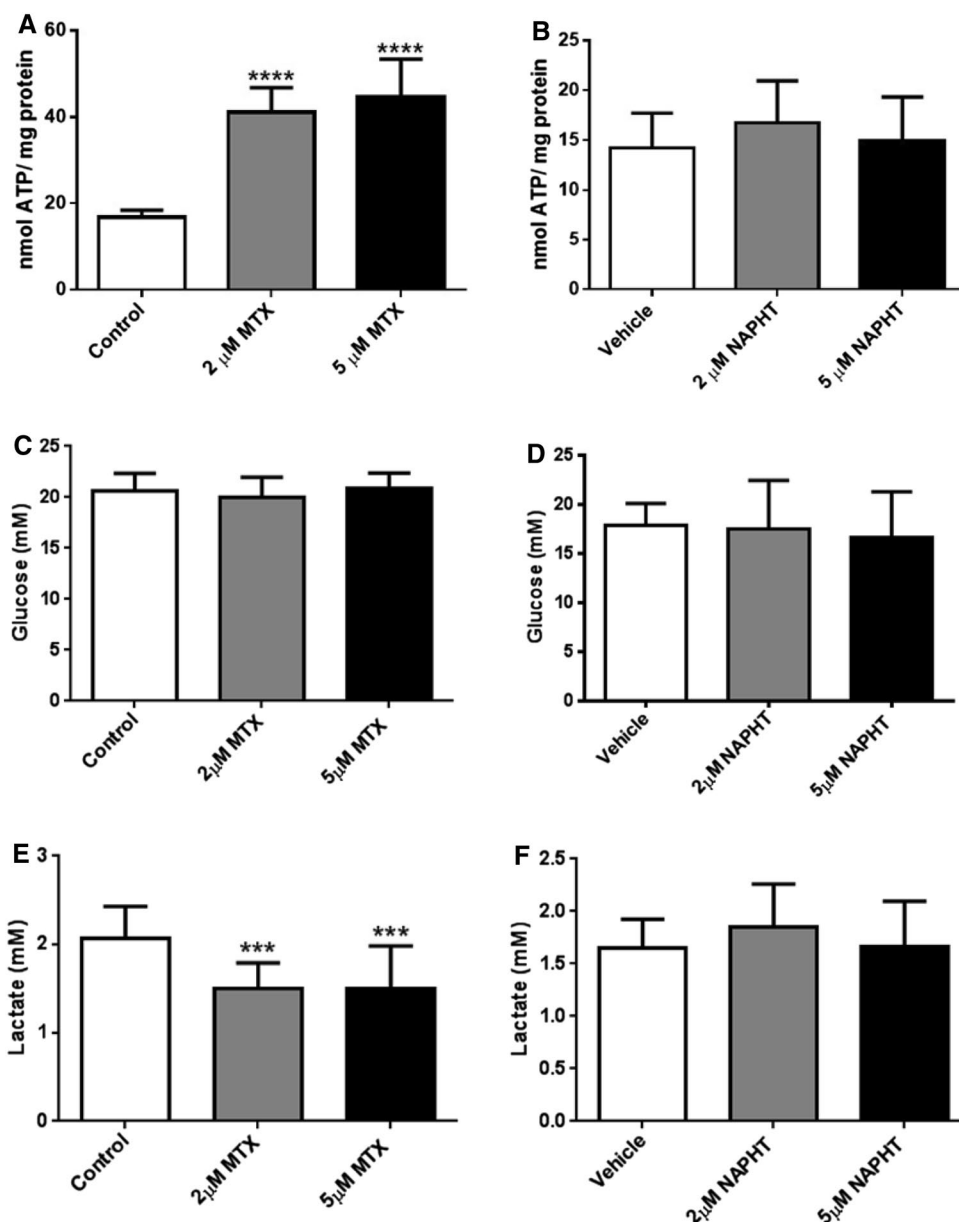
To assess the role of autophagy on NAPHT-induced cytotoxicity, the lysosomal uptake of NR was evaluated in cells exposed to 2 μM NAPHT and 3-methyladenine. At 48 h, 3-methyladenine caused a partial protection against NAPHT-induced cytotoxicity (Fig. 10b).

Moreover, *N*-acetyl cysteine, at 1 mM, increased cell death caused by 2 μM NAPHT, at 48 h (Fig. 10c). The use of *N*-acetyl cysteine per se at 1 mM did not cause significant change in cellular viability when compared to vehicle-incubated cells (DMSO 0.1 % v/v).

Discussion

This work, to the best of our knowledge, is the first to make a broad study of MTX cytotoxicity in differentiated H9c2

Fig. 8 ATP intracellular levels (a, b), glucose (c, d) and lactate (e, f) medium levels. Results of ATP levels in differentiated H9c2 cells incubated with 2 and 5 μ M of MTX (a) or NAPHT (b) for 24 h are expressed in nmol ATP/mg protein and are presented as mean \pm SD of six independent experiments. Results of glucose (c, d) and lactate (e, f) medium levels after a 24-h incubation of 2 and 5 μ M MTX or NAPHT are expressed in mM and are presented as mean \pm SD of nine independent experiments (14 wells) for MTX and four independent experiments for NAPHT (4 wells). DMSO (final concentration of 0.1 % v/v) was used as vehicle in NAPHT-incubated cells. Statistical analyses were performed using the ANOVA test, followed by the Tukey's post hoc test (*** p < 0.001; **** p < 0.0001 vs. control)



cells and to perform a wide range of evaluations concerning the metabolite, NAPHT. Extensive concentration-dependent cytotoxicity caused by MTX affected mitochondrial and energetic pathways, namely with up-regulation of ATP synthase activity, decreased lactate in the media, and mitochondrial membrane potential depolarization at different time-points. Most importantly, the NAPHT metabolite of MTX, often linked to MTX's pharmacological anticancer properties, was less cardiotoxic in this in vitro model when using equimolar concentrations. Even so, both molecules share the potential ability to activate autophagy in this cellular model.

The most commonly used cytotoxicity assays were employed to assess MTX toxicity in vitro. The results obtained are complementary and allow a better characterization of the

putative cytotoxic mechanisms involved, because of the different natures of each assay (Fotakis and Timbrell 2006). Cells incubated with MTX (0.01–5 μ M) showed time- and concentration-dependent cytotoxicity, and the NR assay was the most sensitive for MTX-induced cytotoxicity. In the work carried out by Rossato and co-workers, several MTX concentrations and time-points were tested using undifferentiated H9c2 cells as the in vitro model (Rossato et al. 2013b). With the differentiated H9c2 cells used in the present study, we observed that at 24 h, 1 μ M MTX caused significant decreases in the cells' viability (64.08 ± 8.26 %), whereas in the study by Rossato, the same concentration did not lead to significant cell death in undifferentiated H9c2 cells at the same time-point and using the same assay, the LDH leakage

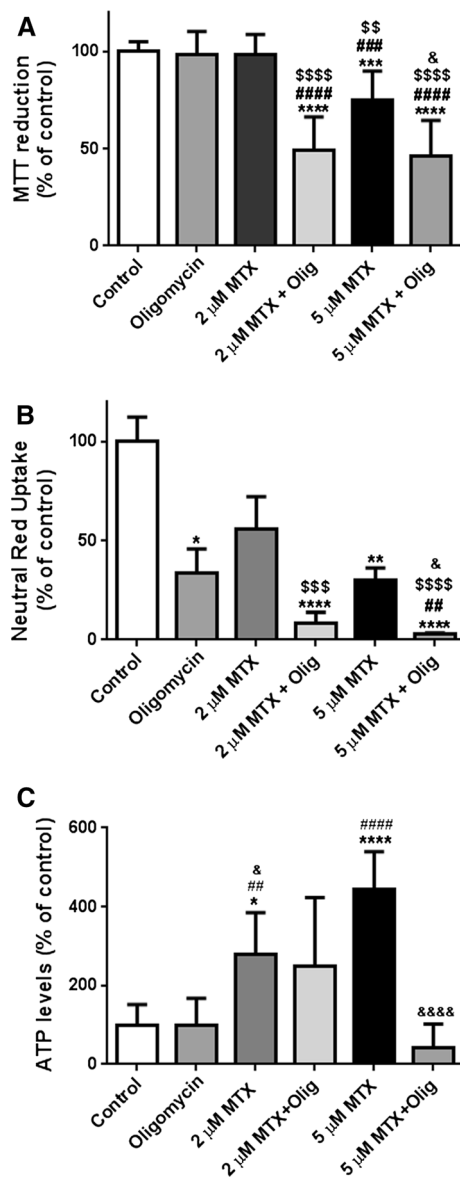


Fig. 9 Mitochondrial dysfunction evaluated by MTT reduction assay (a), NR uptake assay (b) and % of ATP (c) levels in differentiated H9c2 cells incubated with 2 and 5 μM of MTX for 24 h with or without the ATP synthase inhibitor, oligomycin (5 μM final concentration). **a** % MTT reduction results are presented as mean \pm SD of 6–7 independent experiments (24–28 wells). **b** % NR uptake assay results are presented as mean \pm SD of 3 independent experiments (12 wells). **c** % of control ATP levels was obtained of 6–8 independent experiments. Statistical analyses performed: **a, b** Kruskal–Wallis test, followed by the Dunn’s post hoc test or **c** ANOVA test, followed by the Tukey’s post hoc test (* $p < 0.05$; ** $p < 0.01$; *** $p < 0.001$; **** $p < 0.0001$ vs. control; ## $p < 0.01$; ### $p < 0.001$; #### $p < 0.0001$ vs. oligomycin; \$\$ $p < 0.01$; \$\$\$ $p < 0.001$; \$\$\$\$. $p < 0.0001$ vs. 2 μM MTX; & $p < 0.05$; &&& $p < 0.0001$ vs. 5 μM MTX)

assay (Rossato et al. 2013b). Also, at the higher concentration and longer time-point (5 μM at 48 h), we observed increased cell death when compared to undifferentiated H9c2 cells. Despite the lower cellular division rate in differentiated cells,

MTX was more cytotoxic for the cells with the cardiac phenotype; thus, MTX does not act only on cellular division and, in fact, its cytotoxicity appears to be phenotype-specific. In our work, when using the MTT reduction assay, the cytotoxicity observed apparently was lower than what was observed in the study by Rossato et al. (2013b). Actually, the differentiated cells have substantial lower proliferation rate, whereas undifferentiated H9c2 cells are rapidly dividing cells (Rossato et al. 2013b); this fact largely influences the results, since the values obtained in the MTT reduction assay are the result of the ratio of values to control cells whose values largely increase in rapidly dividing cells. Moreover, to the best of our knowledge, there are no previous studies using the NR uptake assay in H9c2 cells (differentiated or not) exposed to MTX. This assay was the most sensitive for the MTX-induced toxicity in differentiated H9c2 cells, when compared with the MTT reduction and the LDH leakage assay, thus showing lysosomes as a new putative cellular target of MTX toxicity.

A common feature of MTX and other topoisomerase II inhibitors is apoptosis promotion, and several works clearly demonstrate that MTX is a pro-apoptotic agent, when using caspase 3 activity assay (Rossato et al. 2013b), or by DAPI staining, Western blot cytochrome *c* release, and the TUNEL assay (Kluza et al. 2004). These studies used μM range concentrations and undifferentiated H9c2 cells, while in our work, no apoptotic signs were observed in 7-day differentiated H9c2 cells. It seems clear that the presence of MTX in fast dividing cells promotes apoptosis, whereas in our study using 7-day differentiated cells, no signs of apoptosis, evaluated by Hoechst and ethidium bromide/acridine stainings, were seen at the time-points tested. Still, the MTX-induced mitochondrial toxicity seems independent of the cellular model. In the present study, lower levels of mitochondrial membrane potential resulting from a 12-h exposure to MTX were observed, suggesting the depolarization of mitochondrial membrane. This depolarization was concentration-dependent. In non-differentiated H9c2 cells, and using other time-points, MTX caused both hyperpolarization and depolarization (Kluza et al. 2004; Rossato et al. 2013b). The mitochondrial changes, including variations in mitochondrial membrane potential, are key events during drug-induced apoptosis; however, the caspase inhibitor was not able to decrease the MTX-induced cytotoxicity, and, as mentioned, no signs of apoptosis were observed.

The cardiotoxicity of MTX has often been linked to its mitochondrial toxicity (Kluza et al. 2004; Rossato et al. 2013b, 2014). In fact, we observed that depolarization of mitochondrial membrane is a rapid phenomenon in MTX-incubated cells, as seen after a 12-h incubation. However, at 24 h, the levels of ATP in the surviving MTX-incubated cells increased, as a result of the increase in ATP synthase activity. Therefore, the mitochondrial depolarization may be transient or the increase in ATP synthase activity by

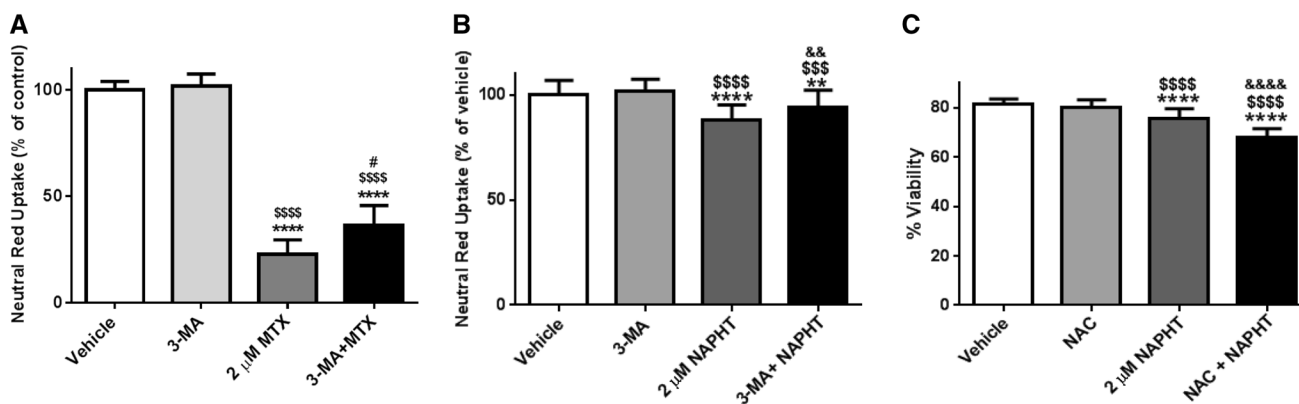


Fig. 10 **a** NR uptake (% of vehicle) in differentiated H9c2 cells incubated with 2 μ M of MTX, 3-methyladenine (3-MA) 2.5 mM and 3-MA + MTX for 48 h. **b** NR uptake assay (% of vehicle) in differentiated H9c2 cells incubated with 2 μ M of NAPHT, 3-MA 2.5 mM and 3-MA + NAPHT for 48 h. **c** Cellular viability at 48 h evaluated by the LDH leakage assay (% of extracellular LDH/total LDH) in differentiated H9c2 cells incubated with 2 μ M of NAPHT and *N*-acetyl cysteine (NAC), an antioxidant, at 1 mM. DMSO (final con-

centration of 0.1 % v/v) was used as vehicle for NAPHT. Results are mean \pm SD of 7 independent experiments (42 wells) in **a**, of 5 independent experiments (30 wells) in **b** and 4 independent experiments (total of 24 wells) in **c**. Statistical analyses performed: **a** Kruskal–Wallis test, followed by the Dunn’s post hoc test or **b**, **c** ANOVA test, followed by the Tukey’s post hoc test (** $p < 0.01$; **** $p < 0.0001$ vs. vehicle; \$\$\$ $p < 0.001$; \$\$\$\$ $p < 0.0001$ vs. 3-MA or NAC; & $p < 0.05$; && $p < 0.01$; &&&& $p < 0.0001$ vs. 2 μ M MTX or NAPHT)

itself causes cellular depolarization. The increase in cardiac ATP synthase activity after MTX was already observed *in vivo* in rats exposed to MTX (Rossato et al. 2014). In addition, when pre-incubating with oligomycin, an ATP synthase inhibitor, we showed that ATP levels decreased significantly in the 5 μ M MTX condition, which also resulted in an increase in the MTX-induced cytotoxicity observed. Then, we can assume that the increase in ATP levels may be an adaptation response, functioning as an attempt to guarantee the cells’ survival.

After cellular uptake, glucose is activated and through glycolysis a molecule of glucose is degraded in a series of enzyme-catalysed reactions to yield pyruvate and NADH/H⁺ in the cytosol. Also, lactate can be converted into pyruvate, in a reversible catalysed reaction in the cytosol. In the mitochondria, pyruvate undergoes oxidation to acetyl-CoA that enters the tricarboxylic acid cycle where NADH/H⁺ and FADH₂ are generated. These electron donors enter the electron transporter chain to form ATP and water (Costa et al. 2009b). In the present work, MTX decreased lactate levels, presumably due to increased conversion of lactate to pyruvate. The increase in pyruvate levels may contribute to the altered mitochondrial status, namely the increase in ATP synthase activity. The increase in ATP synthase activity was conceivably responsible for the dissipation of mitochondrial membrane potential that can be even more pronounced if accompanied by malfunction of other mitochondrial complexes. In fact, in the heart of MTX-treated rats, the mitochondrial complexes, depending on the time-frame of animal sacrifice after the same cumulative dose of MTX, have different behaviours regarding their activity (Rossato et al. 2014).

Another type of cell death induced by MTX was identified in the present work. Actually, autophagy seems at least partially involved in MTX-induced toxicity in this cellular model. Autophagy is characterized by the formation of vacuoles in the cytoplasm of cells that are dying with the degradation of cytoplasmic components within lysosomes (Soares et al. 2014). It is known that MTX is able to largely accumulate within the cells cytoplasm, increasing several fold over its extracellular concentrations (Feofanov et al. 1997a; Smith et al. 1992). Moreover, MTX has lysosomotropic properties on cancer cells (Diétel et al. 1990; Ndolo et al. 2012). Lysosomes sequester lipophilic amine drugs, like MTX, through a non-enzymatic and non-transporter mediated process. Lipophilic amine drugs with weak-base properties readily diffuse across cell membranes at physiologic pH via passive diffusion. However, upon entry into acidic lysosomes and later into endosomes, they undergo protonation and are hence entrapped in lysosomes in their cationic state (Goldman et al. 2009). The involvement of autophagy in MTX-induced cardiotoxicity has never been reported; even so the cytoplasmic vacuolization has been described in the heart after MTX administration to mice (Dores-Sousa et al. 2015), and *in vitro* in neonatal rat cardiomyocytes exposed to MTX (Shipp et al. 1993). Nonetheless, the nature of those vesicles was not characterized in those works. Presently, we were able to observe several dark vacuoles in the surviving cells incubated with MTX, and the autophagy inhibitor used, 3-methyladenine, was able to give a partial protection in the NR assay. The lack of total reversion shows that other mechanisms are involved in MTX cytotoxicity.

Data regarding MTX metabolism are very scarce (Reis-Mendes et al. 2015), and information on MTX’s

metabolites and their cardiotoxicity is practically non-existent, with only one work already published (Shipp et al. 1993). In the present study, we synthesized the MTX metabolite, NAPHT, since it is not commercially available. That synthesis was undertaken by an HRP catalysed H_2O_2 oxidation. Several derivatives were observed by chromatographic analysis of the crude product, and one purified derivative was isolated and identified as NAPHT. The enzymatically catalysed oxidation of MTX by HRP/ H_2O_2 has already been demonstrated in other works (Reszka et al. 1986; Kolodziejczyk et al. 1988; Bruck and Bruck 2011), but only in a very few works was the isolation NAPHT achieved and partially characterized by ^{13}C NMR and liquid chromatography-mass spectrometry. In the study by Blanz et al. (1991), NAPHT was isolated by preparative HPLC from the urine of a patient, and it was characterized by tandem mass spectrometry and UV–visible spectroscopy. The proposed mechanism for the formation of NAPHT (seen in Fig. 1b; Blanz et al. 1991) established the reaction to proceed via a two-electron oxidation of the phenylenediamine substructure I to the formation of the highly reactive quinone II. The non-protonated form termed IV of the equilibrium reacts by an intramolecular attack of the basic amino group of the side chain with the electrophilic centre at C-6 of MTX radical cation. Subsequent oxidation of the cyclized radical V led to the formation of NAPHT. Herein, with the purification methods used, it was possible to obtain a high-purity NAPHT product that allowed further toxicological evaluation.

As mentioned previously, works focusing on NAPHT are very scarce and do not usually involve the potential cardiotoxic effects (Feofanov et al. 1997a, b; Panousis et al. 1994, 1997). NAPHT, like MTX, is distributed throughout the cytoplasm of K562 cells (Feofanov et al. 1997a, b). In fact, Feofanov and colleagues demonstrated, in living K562 cells, that MTX and NAPHT are presumably localized within mitochondria or at least in their proximity (Feofanov et al. 1997a). Also, NAPHT formed by the oxidation of MTX by activated human neutrophils is able to bind to DNA (Panousis et al. 1997). Regarding its cytotoxicity, when isolated neonatal rat heart myocytes were exposed for 3 h to NAPHT (followed by a 72-h free drug period), it was revealed that the metabolite had *circa* 20 times lower cytotoxicity than MTX to myocytes (Shipp et al. 1993). Indeed, we also observed that MTX was more cytotoxic than the metabolite NAPHT, although they share similar features, like early mitochondrial depolarization. Additionally, both MTX and NAPHT seem to activate autophagy, as the inhibitor, 3-methyladenine, partially reverted the observed cytotoxicity. The chemical nature of these molecules, namely their common characteristics as hydrophobic weak bases, seems to

influence the activation of that pathway (Zhitomirsky and Assaraf 2015). On the other hand, NAPHT did not change the energetic parameters in the differentiated H9c2 cells after a 24-h exposure period. Interestingly, NAPHT had its cytotoxicity increased after the pre-incubation with *N*-acetyl cysteine, a powerful antioxidant. It is known that small amounts of oxidative stress can create a state of pre-conditioning that increases cell chances of survival (Costa et al. 2009a). Although the mechanisms are not clear so far, the *N*-acetyl cysteine seems to impair the pre-conditioning state elicited by NAPHT in differentiated H9c2 cells; therefore, their co-incubation elicits a higher cell death.

In conclusion, this work is the first to make a broad study of MTX in differentiated H9c2 cells and to perform a wide range of evaluations with one of its most relevant metabolites in humans, NAPHT. Most importantly, the NAPHT metabolite of MTX, often associated with the pharmacological anticancer properties of MTX, was shown to be less cardiotoxic in this *in vitro* model. If proven that NAPHT has similar anticancer properties and lower cardiotoxicity when compared to MTX, it should be regarded as an interesting option as a safer anticancer drug.

Acknowledgments We would like to thank Dr. Sara Cravo for her technical assistance in obtaining the HPLC—diode array detector data and Centro de Apoio Científico e Tecnológico à Investigação (CACTI, University of Vigo, Spain) for enabling measurements at the API III mass spectrometer. NMR data was collected at the UC-NMR facility which is supported in part by FEDER—European Regional Development Fund through the COMPETE Programme (Operational Programme for Competitiveness) and by National Funds through FCT—Fundação para a Ciência e a Tecnologia (Portuguese Foundation for Science and Technology) through grants RECI/QEQ-QFI/0168/2012, CENTRO-07-CT62-FEDER-002012, and Rede Nacional de Ressonância Magnética Nuclear (RNRMN). This work was supported by the Fundação para a Ciência e Tecnologia (FCT)—projects EXPL/DTP-FTO/0290/2012 and PTDC/DTP-FTO/1489/2014—QREN initiative with EU/FEDER financing through COMPETE—Operational Programme for Competitiveness Factors and partially supported by the Strategic Funding UID/Multi/04423/2013 through national funds provided by FCT—Foundation for Science and Technology and European Regional Development Fund (ERDF), in the framework of the programme PT2020. The authors are also grateful to “Fundação para a Ciência e a Tecnologia” for Grant Nos. UID/MULTI/04378/2013 and UID/Multi/04423/2013, ERDF, and PT2020. V.M.C. (Post doc) acknowledges “Fundação para a Ciência e Tecnologia (FCT)” for her post doc Grants (SFRH/BPD/63746/2009 and SFRH/BPD/110001/2015).

References

- Albini A, Pennesi G, Donatelli F, Cammarota R, De Flora S, Noonan DM (2010) Cardiotoxicity of anticancer drugs: the need for cardio-oncology and cardio-oncological prevention. *J Natl Cancer Inst* 102(1):14–25
- Allemani C, Weir HK, Carreira H et al (2015) Global surveillance of cancer survival 1995–2009: analysis of individual data for

- 25,676,887 patients from 279 population-based registries in 67 countries (CONCORD-2). *The Lancet* 385(9972):977–1010
- Avasaraala JR, Cross AH, Clifford DB, Singer BA, Siegel BA, Abbey EE (2003) Rapid onset mitoxantrone-induced cardiotoxicity in secondary progressive multiple sclerosis. *Mult Scler* 9(1):59–62
- Blanz J, Mewes K, Ehninger G et al (1991) Evidence for oxidative activation of mitoxantrone in human, pig, and rat. *Drug Metab Dispos* 19(5):871–880
- Bruck TB, Bruck DW (2011) Oxidative metabolism of the anti-cancer agent mitoxantrone by horseradish, lacto- and lignin peroxidase. *Biochimie* 93:217–226
- Bruck TB, Harvey PJ (2003) Oxidation of mitoxantrone by lactoperoxidase. *Biochim Biophys Acta* 1649:154–163
- Capela JP, Meisel A, Abreu AR et al (2006) Neurotoxicity of Ecstasy metabolites in rat cortical neurons, and influence of hyperthermia. *J Pharmacol Exp Ther* 316(1):53–61
- Capela JP, da Costa Araujo S, Costa VM et al (2013) The neurotoxicity of hallucinogenic amphetamines in primary cultures of hippocampal neurons. *Neurotoxicology* 34:254–263
- Carver JR, Desai CJ (2010) Cardiovascular toxicity of antitumor drugs: dimension of the problem in adult settings. In: Minotti G (ed) *Cardiotoxicity of non-cardiovascular drugs*. Wiley, Hoboken, pp 127–199
- Chiccarelli FS, Morrison JA, Cosulich DB et al (1986) Identification of human urinary mitoxantrone metabolites. *Cancer Res* 46(9):4858–4861
- Coleman RE, Maisey MN, Knight RK, Rubens RD (1984) Mitoxantrone in advanced breast cancer—a phase II study with special attention to cardiotoxicity. *Eur J Cancer Clin Oncol* 20(6):771–776
- Costa VM, Silva R, Ferreira LM et al (2007) Oxidation process of adrenaline in freshly isolated rat cardiomyocytes: formation of adrenochrome, quinoproteins, and GSH adduct. *Chem Res Toxicol* 20(8):1183–1191
- Costa VM, Silva R, Ferreira R et al (2009a) Adrenaline in pro-oxidant conditions elicits intracellular survival pathways in isolated rat cardiomyocytes. *Toxicology* 257(1–2):70–79
- Costa VM, Silva R, Tavares LC et al (2009b) Adrenaline and reactive oxygen species elicit proteome and energetic metabolism modifications in freshly isolated rat cardiomyocytes. *Toxicology* 260(1–3):84–96
- Dietel M, Arps H, Lage H, Niendorf A (1990) Membrane vesicle formation due to acquired mitoxantrone resistance in human gastric carcinoma cell line EPG85-257. *Cancer Res* 50(18):6100–6106
- Dores-Sousa JL, Duarte JA, Seabra V, Bastos ML, Carvalho F, Costa VM (2015) The age factor for mitoxantrone's cardiotoxicity: multiple doses render the adult mouse heart more susceptible to injury. *Toxicology* 329:106–119
- Ehninger G, Schuler U, Proksch B, Zeller KP, Blanz J (1990) Pharmacokinetics and metabolism of mitoxantrone. A review. *Clin Pharmacokinet* 18(5):365–380
- Feofanov A, Sharonov S, Fleury F, Kudelina I, Nabiev I (1997a) Quantitative confocal spectral imaging analysis of mitoxantrone within living K562 cells: intracellular accumulation and distribution of monomers, aggregates, naphthoquinoxaline metabolite, and drug-target complexes. *Biophys J* 73(6):3328–3336
- Feofanov A, Sharonov S, Kudelina I, Fleury F, Nabiev I (1997b) Localization and molecular interactions of mitoxantrone within living K562 cells as probed by confocal spectral imaging analysis. *Biophys J* 73(6):3317–3327
- Ferlay J, Steliarova-Foucher E, Lortet-Tieulent J et al (2013) Cancer incidence and mortality patterns in Europe: estimates for 40 countries in 2012. *Eur J Cancer* 49(6):1374–1403
- Ferreira PS, Nogueira TB, Costa VM et al (2013) Neurotoxicity of “ecstasy” and its metabolites in human dopaminergic differentiated SH-SY5Y cells. *Toxicol Lett* 216(2–3):159–170
- Fotakis G, Timbrell JA (2006) In vitro cytotoxicity assays: comparison of LDH, neutral red, MTT and protein assay in hepatoma cell lines following exposure to cadmium chloride. *Toxicol Lett* 160(2):171–177
- Freitas M, Costa VM, Ribeiro D et al (2013) Acetaminophen prevents oxidative burst and delays apoptosis in human neutrophils. *Toxicol Lett* 219(2):170–177
- Goldman SDB, Funk RS, Rajewski RA, Krise JP (2009) Mechanisms of amine accumulation in, and egress from, lysosomes. *Bioanalysis* 1(8):1445–1459
- Gupta MK, Neelakantan TV, Sanghamitra M et al (2006) An assessment of the role of reactive oxygen species and redox signaling in norepinephrine-induced apoptosis and hypertrophy of H9c2 cardiac myoblasts. *Antioxid Redox Signal* 8(5–6):1081–1093
- Kimes BW, Brandt BL (1976) Properties of a clonal muscle cell line from rat heart. *Exp Cell Res* 98(2):367–381
- Kluza J, Marchetti P, Gallego M-A et al (2004) Mitochondrial proliferation during apoptosis induced by anticancer agents: effects of doxorubicin and mitoxantrone on cancer and cardiac cells. *Oncogene* 23(42):7018–7030
- Kolodziejczyk P, Reszka K, Lown JW (1988) Enzymatic oxidative activation and transformation of the antitumor agent mitoxantrone. *Free Radic Biol Med* 5:13–25
- Martins JB, Bastos Mde L, Carvalho F, Capela JP (2013) Differential effects of methyl-4-phenylpyridinium ion, rotenone, and paraquat on differentiated SH-SY5Y cells. *J Toxicol* 2013:347312
- Menna P, Salvatorelli E, Minotti G (2008) Cardiotoxicity of antitumor drugs. *Chem Res Toxicol* 21(5):978–989
- Mewes K, Blanz J, Ehninger G, Gebhardt R, Zeller KP (1993) Cytochrome P-450-induced cytotoxicity of mitoxantrone by formation of electrophilic intermediates. *Cancer Res* 53(21):5135–5142
- Ndolo RA, Luan Y, Duan S, Forrest ML, Krise JP (2012) Lysosomotropic properties of weakly basic anticancer agents promote cancer cell selectivity in vitro. *PLoS ONE* 7(11):e49366
- Panousis C, Kettle AJ, Phillips DR (1994) Oxidative metabolism of mitoxantrone by the human neutrophil enzyme myeloperoxidase. *Biochem Pharmacol* 48(12):2223–2230
- Panousis C, Kettle AJ, Phillips DR (1997) Neutrophil-mediated activation of mitoxantrone to metabolites which form adducts with DNA. *Cancer Lett* 113(1–2):173–178
- Pereira SL, Ramalho-Santos J, Branco AF, Sardao VA, Oliveira PJ, Carvalho RA (2011) Metabolic remodeling during H9c2 myoblast differentiation: relevance for in vitro toxicity studies. *Cardiovasc Toxicol* 11(2):180–190
- Pratt CB, Vietti TJ, Etcubanas E et al (1986) Novantrone for childhood malignant solid tumors. A pediatric oncology group phase II study. *Invest New Drugs* 4(1):43–48
- Reis-Mendes A, Sousa E, Bastos ML, Costa VM (2015) Metabolism of anticancer drugs and cardiotoxicity: a missing link? *Curr Drug Metab* 17(1):75–90
- Reszka KJ, Chignell CF (1996) Acid-catalyzed oxidation of the anticancer agent mitoxantrone by nitrite ions. *Mol Pharmacol* 50:1612–1618
- Reszka K, Kolodziejczyk P, Lown JW (1986) Horseradish peroxidase-catalyzed oxidation of mitoxantrone: spectrophotometric and electron paramagnetic resonance studies. *J Free Radic Biol Med* 2:25–32
- Rossato LG, Costa VM, de Pinho PG et al (2013a) The metabolic profile of mitoxantrone and its relation with mitoxantrone-induced cardiotoxicity. *Arch Toxicol* 87:1809–1820
- Rossato LG, Costa VM, Vilas-Boas V et al (2013b) Therapeutic concentrations of mitoxantrone elicit energetic imbalance in H9c2 cells as an earlier event. *Cardiovasc Toxicol* 13(4):413–425
- Rossato LG, Costa V, Dallegrave E et al (2014) Mitochondrial cumulative damage induced by mitoxantrone: late onset cardiac energetic impairment. *Cardiovasc Toxicol* 14(1):30–40

- Ruiz M, Courilleau D, Jullian JC et al (2012) A cardiac-specific robotized cellular assay identified families of human ligands as inducers of PGC-1alpha expression and mitochondrial biogenesis. *PLoS ONE* 7(10):e46753
- Seiter K (2005) Toxicity of the topoisomerase II inhibitors. *Expert Opin Drug Saf* 4(2):219–234
- Shi J, Shen HM (2008) Critical role of Bid and Bax in indirubin-3'-monoxime-induced apoptosis in human cancer cells. *Biochem Pharmacol* 75(9):1729–1742
- Shipp NG, Dorr RT, Alberts DS, Dawson BV, Hendrix M (1993) Characterization of experimental mitoxantrone cardiotoxicity and its partial inhibition by ICRF-187 in cultured neonatal rat heart cells. *Cancer Res* 53(3):550–556
- Smith PJ, Sykes HR, Fox ME, Furlong IJ (1992) Subcellular distribution of the anticancer drug mitoxantrone in human and drug-resistant murine cells analyzed by flow cytometry and confocal microscopy and its relationship to the induction of DNA damage. *Cancer Res* 52(14):4000–4008
- Soares AS, Costa VM, Diniz C, Fresco P (2013) Potentiation of cytotoxicity of paclitaxel in combination with CI-IB-MECA in human C32 metastatic melanoma cells: a new possible therapeutic strategy for melanoma. *Biomed Pharmacother* 67(8):777–789
- Soares AS, Costa VM, Diniz C, Fresco P (2014) Combination of CI-IB-MECA with paclitaxel is a highly effective cytotoxic therapy causing mTOR-dependent autophagy and mitotic catastrophe on human melanoma cells. *J Cancer Res Clin Oncol* 140(6):921–935
- Zhitomirsky B, Assaraf YG (2015) Lysosomal sequestration of hydrophobic weak base chemotherapeutics triggers lysosomal biogenesis and lysosome-dependent cancer multidrug resistance. *Oncotarget* 6(2):1143–1156